Quaternary Science Reviews 186 (2018) 123–141

Contents lists available at ScienceDirect

Quaternary Science Reviews

journal homepage: www.elsevier.com/locate/quascirev

A rhinocerotid-dominated megafauna at the MIS6-5 transition: The late Middle Pleistocene Coc Muoi assemblage, Lang Son province, Vietnam

Anne-Marie Bacon [a, *], Pierre-Olivier Antoine [b], Nguyen Thi Mai Huong [c], Kira Westaway [d], Nguyen Anh Tuan [c], Philippe Duringer [e], Jian-xin Zhao [f], Jean-Luc Ponche [g], Sam Canh Dung [h], Truong Huu Nghia [c], Tran Thi Minh [c], Pham Thanh Son [i], Marc Boyon [e], Nguyen Thi Kim Thuy [c], Amandine Blin [j], Fabrice Demeter [k, l]

[a] AMIS Anthropologie moléculaire et imagerie de synthèse, UMR 5288 du CNRS, Université Paris Descartes, Faculté de chirurgie dentaire, 1 rue Maurice Arnoux, 92120 Montrouge, France
[b] Institut des Sciences de l'Évolution, Université Montpellier 2, (CNRS, IRD), CC064, Place Eugène Bataillon, 34095 Montpellier, France
[c] Anthropological and palaeoenvironmental Department, Institute of Archaeology, 61 Phan Chu Trinh Street, Hoan Kiem district, Ha Noi, Viet Nam
[d] 'Traps' MQ Luminescence Dating Facility, Dept Environmental Sciences, Macquarie University, Sydney, NSW 2109, Australia
[e] Ecole et Observatoire des Sciences de la Terre, Institut de Physique du Globe de Strasbourg, CNRS, UMR 7516, Université de Strasbourg, 1 rue Blessig, 67084 Strasbourg, France
[f] Radiogenic Isotope Facility, School of Earth and Environmental Sciences, The University of Queensland, Brisbane, QLD 4072, Australia
[g] ICPEES / LIVE / DYLBAS, Institut de Géologie, Université de Strasbourg, 1 rue Blessig, 67084 Strasbourg, France
[h] Lang Son museum, 2 Hung Vuong Street, Chi Lang district, Lang Son city, Viet Nam
[i] Prehistoric Archaeology Department, Institute of Archaeology, 61 Phan Chu Trinh street, Hoan Kiem district, Ha Noi, Viet Nam
[j] Outils et Méthodes de la Systématique Intégrative, OMSI-UMS 2700 CNRS MNHN, Muséum national d'Histoire naturelle, CP26, 57 rue Cuvier, 75231 Paris cedex 05, France
[k] Musée de l'Homme, UMR 7206, 17 Place du Trocadéro, 75116 Paris, France
[l] Center for GeoGenetics, Øster Voldgade 5-7, 1350 Copenhagen K, Denmark

ARTICLE INFO

Article history:
Received 14 September 2017
Received in revised form
11 February 2018
Accepted 16 February 2018

Keywords:
Southeast Asia
Ecosystems
Rhinoceros sondaicus
Hypoplasia
Lida Ajer

ABSTRACT

Little is known about the ecosystems in the north of the Indochinese peninsula at the Middle-Late Pleistocene transition. In this paper, we analyzed the new fauna from Coc Muoi cave, Lang Son province, northeast Vietnam. In comparison with other well-documented faunas from the region, that of Coc Muoi is distinguished by the predominance of rhinoceroses among diverse large-bodied herbivores. The results of the OSL and pIR-IRSL dating of the cave sediments and U-series dating of flowstones indicate a potential age range of 148-117 ka for the fauna (MIS6-5). The analysis of age-at-death distributions of rhinoceroses, wild cattle, sambar deer, and wild pig, does not show any apparent selectivity of age classes. We also focused our study on rhinoceroses, tapirs, and wild cattle by analyzing the prevalence of hypoplastic defects on deciduous and permanent teeth, in an attempt to assess the health status of the taxa during their first years of growth. The health status of large-bodied herbivores (kouprey and rhinoceros) reveals the importance of stressors (biotic and abiotic) in the rainforest environment during a period of marked climatic transition (MIS6-5) in comparison with other MIS5-4 well-documented faunas from the region.

* Corresponding author. UMR 5288 AMIS « Anthropologie moléculaire et imagerie de synthèse », Université Paris Descartes, Faculté de chirurgie dentaire, 1 rue Maurice Arnoux, 92120 Montrouge, France.
E-mail addresses: anne-marie.bacon@parisdescartes.fr (A.-M. Bacon), pierre-olivier.antoine@univ-montp2.fr (P.-O. Antoine), maihuong72@gmail.com (N.T.M. Huong), kira.westaway@mq.edu.au (K. Westaway), nguyenanhtuan_bio@yahoo.com.vn (N.A. Tuan), duringer@unistra.fr (P. Duringer), j.zhao@uq.edu.au (J.-x. Zhao), ponche@unistra.fr (J.-L. Ponche), truonghuunghiakch@gmail.com (T.H. Nghia), tranthiminh86@gmail.com (T.T. Minh), thanhson9119@gmail.com (P.T. Son), marc.boyon@etu.unistra.fr (M. Boyon), thuythien253@yahoo.com (N.T.K. Thuy), amandine.blin@mnhn.fr (A. Blin), demeter@mnhn.fr (F. Demeter).

https://doi.org/10.1016/j.quascirev.2018.02.017
0277-3791/

1. Introduction

Although widespread in the past environments of Southeast Asia, little is known about the foraging abilities of large predators, the solitary tiger and leopard, or the group-living dhole and hyena. What we know however, is that large predators from Pleistocene mammalian communities had access to a larger spectrum of large prey (van Valkenburg et al., 2016). In the north of Indochina (Corbet and Hill, 1992), the structure of the mammalian ecosystems was shaped by the presence of numerous large-bodied herbivores - at least five types of animals >250 kg (tapirs, wild cattle, and rhinoceroses) up to 5000 kg (elephant and stegodont) - which might have composed part of the predators' diets, among either juvenile or adult individuals.

In 2013, on an invitation from the Vietnamese authorities (Institute of Archaeology in Hanoi and Lang Son Museum), we undertook in a collaborative fieldwork the excavation of the Coc Muoi cave, in Lang Son province, north-east Vietnam. Since the 1960's, the Lang Son province has yielded major faunal assemblages (i.e. Tham Khuyen, Tham Hai, and Keo Leng), which have formed the foundation for the biochronology of the Middle to Late Pleistocene in the Indochinese region (Kha, 1976; Long and Du, 1981; Cuong, 1985, 1992; Olsen and Ciochon, 1990; Ciochon and Olsen, 1986, 1991; Schwartz et al., 1994, 1995; Ciochon et al., 1996; Tougard, 1998, 2001). More recently, the faunal assemblages were used as key-references in palaeoecological studies (Tougard and Montuire, 2006; Louys and Meijaard, 2010), and were also used to resolve diagnostic issues regarding the oldest hominines in Asia (Ciochon, 2009).

In this paper, we aim to increase our understanding of the Pleistocene megaherbivore-bearing ecosystems by analyzing the new fauna from Coc Muoi cave which produced an assemblage of several hundred isolated teeth. In comparison with other well-documented faunas from the region, that of Coc Muoi is distinguished by the predominance of rhinoceroses among megaherbivores (Long et al., 1996; Bacon et al., 2008a; Antoine, 2012). We applied single-grain optically stimulated luminescence (SG-OSL) and post-infrared infrared-stimulated luminescence (pIR-IRSL) to the sediment, and U-series dating to the overlying flowstones to provide a time frame for deposition of the faunal remains in the cave. Taxonomic diversity has been defined based on the teeth. Then, we conducted a taphonomic study of the assemblage, in order to assess factors that may have contributed to the composition and preservation of the mammalian assemblage. We used age-at-death distributions of rhinoceroses, wild cattle, sambar deer, and wild pig in an attempt to emphasize potential prey preferences of large predators. We focused our palaeoecological study on rhinoceroses, tapirs, and wild cattle by analyzing the prevalence of hypoplastic defects on teeth. Considering its composition and age, the fauna has the potential to shed light on a guild of megaherbivores in terms of diversity, relative abundance, and health status around the Middle-Late Pleistocene transition.

2. Description of the site

2.1. Location and geological context

The Coc Muoi cave is close to the Chinese border 155 km NNE from Hanoi in the Lang Son province (Fig. 1). The site is located 10 km north from the main town That Khê.

The landscape is composed of limestone hills and tower karsts dated to the "Anthracolitique" (Fromaget, 1931; Deprat et al., 1963) corresponding to Permo-Carboniferous deposits. The local geology is a massive sparitic limestone with low metamorphic processes. The cave is situated in a small isolated hill, around 150 m in diameter and 30 m high that emerges from the cultivated fields 361 m above the sea level. The precise location is N22° 21′ 21.54", E106° 26′ 6.12" (Fig. 2A). The entrance of the cave, hidden in the forest, is situated 10 m above the cultivated plain (Fig. 2B and C).

The chambers within the cave have a total length of 40 m with a NE-SW orientation (Figs. 3 and 4). The narrow cave entrance (≤1 by 1 m) opens out to 4 m long passageway leading to a first chamber of ~12 m (referred to as "upper hall" in Figs. 3B and 4B). A second chamber, named "lower hall", is situated 1.45 m below the upper level (Figs. 3B and 4B). From the lower hall, a small passageway runs below the upper hall partly blocked by clay (Fig. 4B).

The upper hall is characterized by massive concretions, flowstones, stalactites, stalagmites and various other speleothems that overly light brown argillaceous sediment but with minimal fossils. This part has not been exploited. Several trenches were opened in the fossils-rich lower hall which displays two types of deposits (Fig. 5). The center of the cavity is almost entirely filled with moist yellow silty clay. The upper part of this clay (up to 30 cm) is completely reworked by modern digging (clays are exploited by farmers). Some angular limestone clasts from the substratum of the hill are scattered on the surface. Otherwise, large mud cracks cover the greatest part of the surface suggesting episodic cave flooding. These deposits do not contain fossils.

At the periphery of the cave, plastered on the wall, a solid brown to light brown sandy/clayey breccia unit is characterized by a progressive enrichment in calcite from the base to the top of the section with some limestone clasts and quartz pebbles (Fig. 5). A flowstone overlies this breccia section and is composed of two different phases of deposits. The upper part in made by modern stalactites (light green on Fig. 5) which overlies an older flowstone (dark green on Fig. 5) that in turn overlies the breccia. All fossils were discovered in the sediment below this older flowstone (brown color on Figs. 3–5). The stratigraphic relationship between the soft clayey sediment on the surface of the cave and that plastered on the wall at the periphery indicates an erosion surface (Fig. 5). In the passageway that runs below the upper hall (Fig. 4B), the sediment is almost the same as that plastered at the periphery of the cave but with less calcitic cementations, and contains similar fossils.

2.2. Cave history

The history of the filling of the cave is summarized in Fig. 5 with four phases (from old to young). The cave was filled by the sandy/clayey breccia at least half way up the cave wall (phase 1). The water and sediment entered the cave, bringing the sediment and vertebrate remains studied in this paper. Several flowstones were precipitated progressively more frequently and with increasing thickness during this phase. A large section of the deposits from phases 1 and 2 deposition are removed by erosion, and new sediments are deposited via cut and fill processes (phase 3). An obvious erosional surface separates phases 1 and 2 from phase 3. The last deposit in the cave consists of stalactites and plastic clayey sediment (phase 4).

3. Methods and material

3.1. Dating strategy

To constrain the fossil deposition within Coc Muoi cave two sediment samples for luminescence dating (VCOCMU5 and 6) were collected from two areas of the cave within the unconsolidated breccia sediment that is capped by an overlying flowstone. One was sampled from directly below the capping flowstone by the south cave wall (VCOCMU5) and the other from the opposite cave wall at

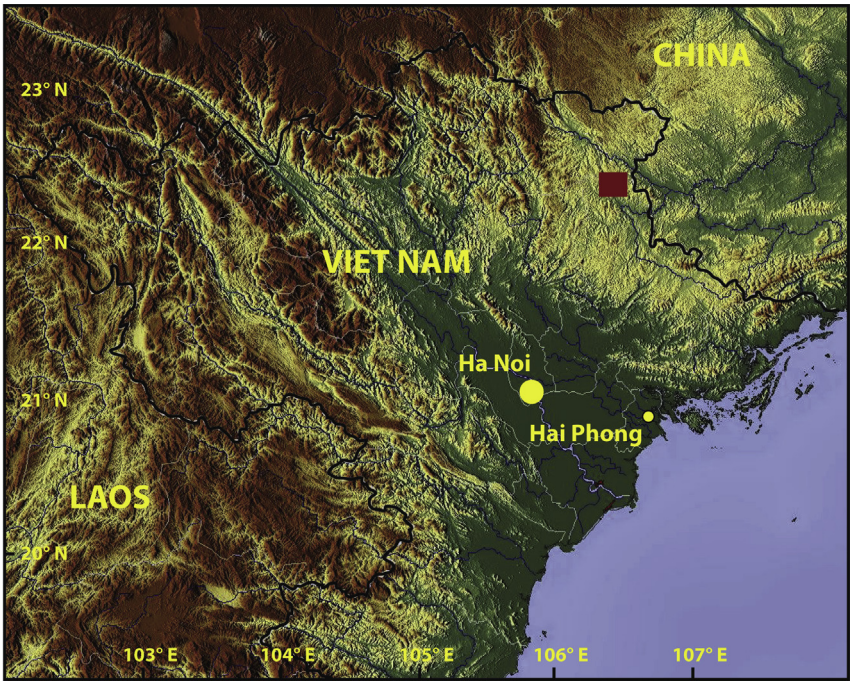

Fig. 1. Map of northern Vietnam with the location of the studied area (red square) in Lang Son province. (For interpretation of the references to color in this figure legend, the reader is referred to the Web version of this article.)

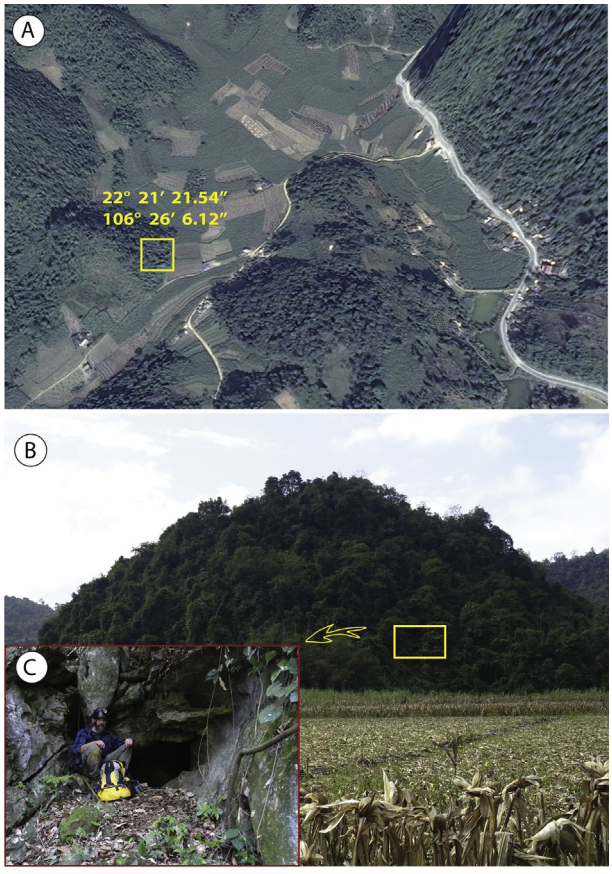

Fig. 2. A. Satellite picture and coordinates of the Coc Muoi karst tower; B. Photo of the limestone hill with the altitude of the cave (yellow square); C. Entrance of the cave. (For interpretation of the references to color in this figure legend, the reader is referred to the Web version of this article.)

around the same height (VCOCMU6) (Fig. 5). The capping flowstone was sampled for U-series dating (VCOCMU-F3 and F4). The single-grain optically stimulated luminescence (SG-OSL) dating of quartz had a very low acceptance rate (1.2–1.5%) resulting in only 39 and 28 accepted grains for samples VCOCMU5 and 6, respectively. As this is much lower than an acceptable statistically significant number of grains we also supplemented this chronology with post-infrared infrared-stimulated luminescence (pIR-IRSL) dating techniques for single-aliquots (SA) of feldspars. This was to take advantage of the higher dose saturation of these minerals (Thompsen et al., 2008; Buylaert et al., 2009; Thiel et al., 2011; Li and Li, 2011, 2012), and to provide a direct comparison and supporting chronology for the quartz results (see Supplementary Information).

3.2. Faunal analysis

3.2.1. References and parameters

Taxa have been identified on the basis of isolated teeth. We followed the taxonomy of Wilson and Reeder (2005). Each tooth or fragment of tooth has been considered as one specimen to estimate NISP (number of identified specimens). MNI (minimum number of individuals) have been based on the frequency (MNIf) of the most common tooth by taxon, and on the combination of data (type of tooth, cohort based on eruption and/or wear stages) (MNIc) (Lyman, 2008).

We analyzed the differential survivorship of teeth (upper *vs* lower; permanent *vs* deciduous). We also observed the chisel marks on roots inflicted by porcupines. Gnawing intensity has been defined using an estimate of the quantity of root gnawed: partially (1/4 to 3/4 of the root) or totally (the root is missing), already used in a previous analysis (Bacon et al., 2015).

The Fisher's exact test performed on data was run in R statistical software version 3.3.2 (https://R-project.org) (R Core Team, 2017). For all statistical tests, we used a level of significance of 5%.

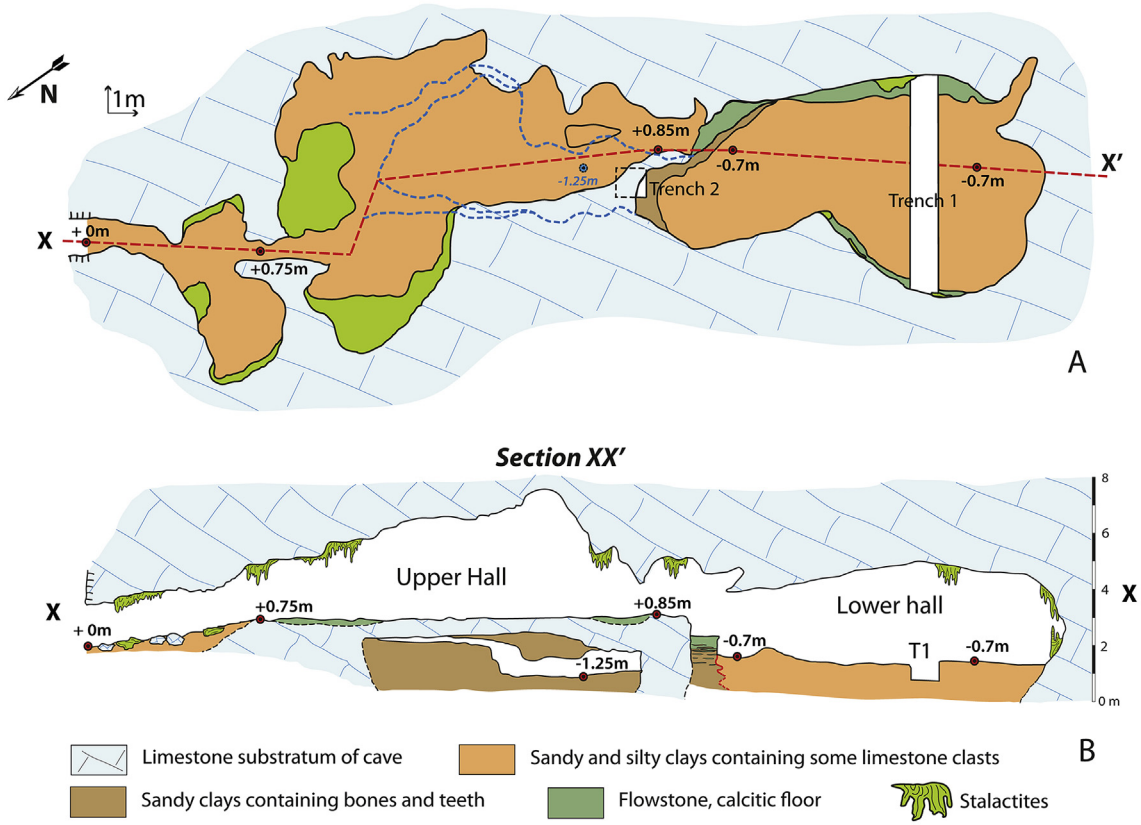

Fig. 3. A. Map of the Coc Muoi cave; B. Vertical section (XX′) of the cave.

3.2.2. Age estimate of individuals of some large-sized species (MNIc)

In relation to *Elephas maximus*, we considered the number of worn lamellae on the grinding occlusal surfaces of lower teeth, and used age reference chart based on modern specimens (Roth and Shoshani, 1988); in relation to felids, the three wear stage of crown (1, "slight", young adult; 2, "moderate", mature adult; 3, "heavy", old adult) (van Valkenburgh, 1988; van Valkenburgh and Hertel, 1993), and in relation to ursids, the nine wear stages of crowns (I-III, juvenile; IV-VII, prime adult; VIII-IX, adult) defined on the brown bear (*Ursus arctos*) (Stiner, 1998).

For building age-at-death distribution of bovids and cervids, we used the amount of crown age reduction of one deciduous tooth and permanent molars m1-m3 (Stiner, 1990; Lyman, 1994; Steele, 2004). Ages of individuals are grouped in large classes defined as 10% of the potential lifespan of species (Klein, 1978). In relation to the suid, we used the crown formation sequences and occlusal surface wear patterns of m1-m3 (Grant, 1982; Rolett and Chiu, 1994) to estimate age classes (Bacon et al., 2015) (see Supplementary Information).

In relation to rhinocerotids, we followed the protocol used in Bacon et al. (2008a), derived from the correspondence between dental wear stages and individual ages in a recent white rhino population, as detailed by Hillman-Smith et al. (1986). Rhinocerotid population structures were then hypothesized by considering three major age classes (juveniles, subadults, and adults), coinciding with the age classes 0-V (0–3 yrs), VI-VIII (3–7 yrs), and IX–XVI (7–40 yrs), respectively.

The Kolmogorov-Smirnov test was performed on mortality profiles of rhinocerotids, using R statistical software version 3.3.2 (https://R-project.org) (R Core Team, 2017).

3.2.3. Prevalence of hypoplastic defects

We conducted a macroscopic analysis of local marks of enamel hypoplasia on deciduous and permanent teeth of large-sized species, *i.e.* rhinoceroses, wild cattle, and tapirs. We did not use microscopy to record the defects, but restricted our analysis to those seen with the unaided eye. Observation on the rhinocerotid sample was quite easy, however that on the large bovid sample was particularly difficult, as numerous crowns are partially recovered by cement. The defects observed on the enamel are of two types: modifications in the thickness of enamel described as pit, furrow, or plane of missing enamel, and changes in the coloration of enamel (Suckling, 1989; Goodman and Rose, 1990). We described the location of defects on the crown height of hypsodont molars of bovids as basal third, middle third, or occlusal third. They are most of the time caused by episodic disruptions during tooth crown formation due to physiological stresses, affecting individuals *in utero* at the first months of their growth or after birth (Hillson, 2005). These defects may be related to undernutrition and diseases, to stressors specific to age, birth, weaning, calf-cow separation, or other factors such as altitude, and climate, often under a combined influence (Goodman and Rose, 1990). In rhinocerotids specifically, this pathology is generally related either to a starving episode for the mother during pregnancy or nursing (when observed on milk teeth) or to undernutrition coinciding with weaning or abandonment of the calf by a newly pregnant mother (when present on permanent teeth; Mead, 1999; Fourvel et al., 2015).

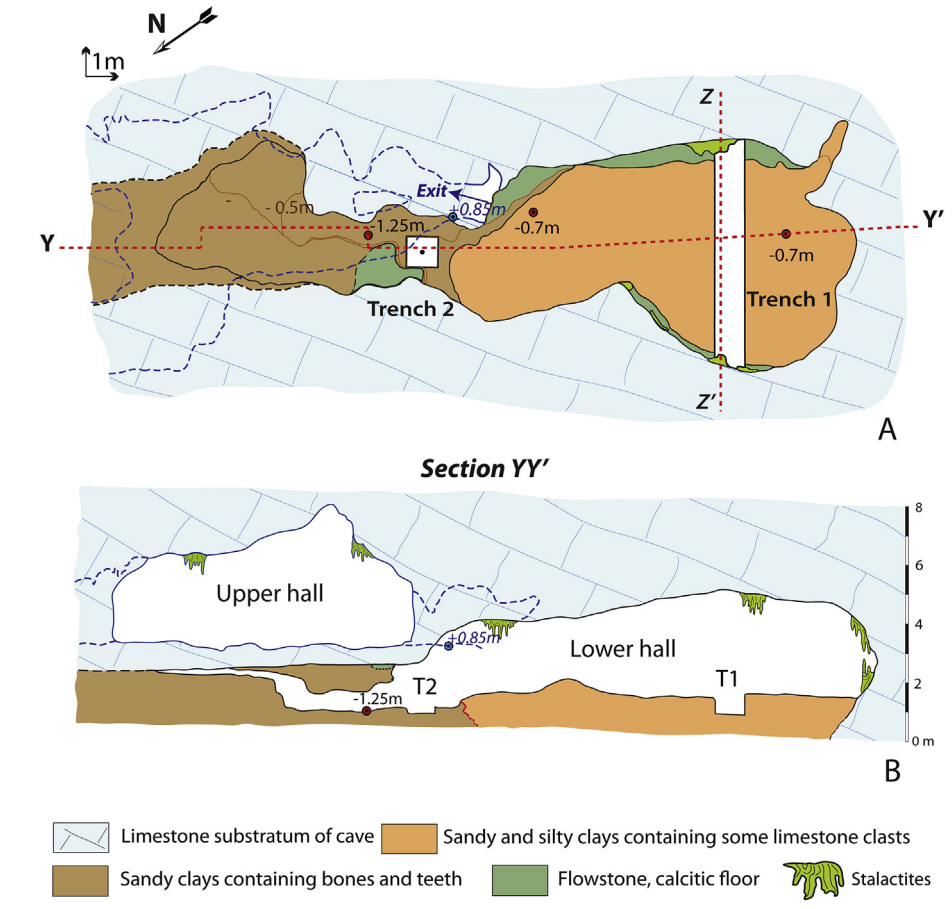

Fig. 4. A. Map of the Coc Muoi cave at the level of the lower hall; B. Vertical section (YY') of the lower hall.

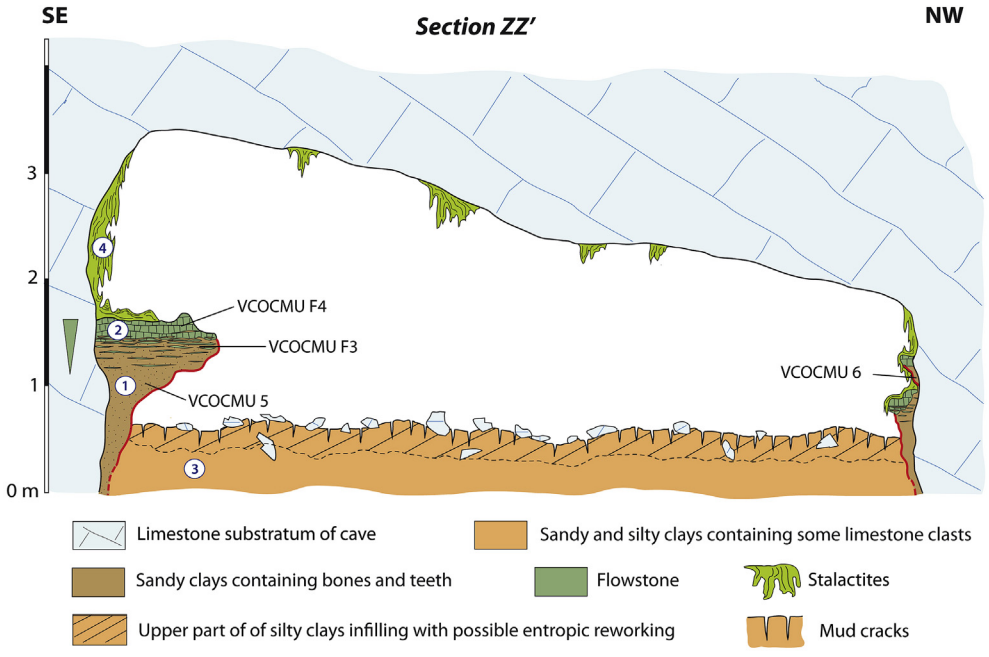

Fig. 5. Vertical section (ZZ') of the Coc Muoi cave, unearthed by trench 1. See Fig. 4 for the precise location of the trench 1 in the lower hall. The location of the samples taken from the overlying flowstones (VCOCMU F3 and F4) for U-series dating and from the breccia unit (VCOCMU 5 and 6) for luminescence dating. Note that the relative height of VCOCMU6 is a projected onto this transect to demonstrate the relationship between the two luminescence samples.

4. Results

4.1. Dating results

The results of both the OSL and pIR-IRSL dating of the cave sediments (VCOCMU5 and 6) indicate that the sediments were deposited in the cave between 148 and 146 (pIR-IRSL) and 125-117 (OSL) ka, with a potential age range of 148-117 ka (Table 1). These results agree within their error margins and also agree with the U-series results that indicate that the overlying flowstone was precipitated between 114 and 108 ka (VCOCMU-F3 and F4) (Table 2), and therefore represents a minimum age for breccia and fossil accumulation.

4.2. Identification of taxa

4.2.1. Artiodactyla

Sixteen teeth belong to a medium-sized cervid, but there is an insufficient number to identify them at a species level. One hundred and fifty teeth and one jaw fragment (CM217) with p3-p4 (NISP = 152) exhibit the morphological pattern and dimensions of *Rusa unicolor* (SI-Table 1). The p4 shows a clear molarization (Heintz, 1970). Dimensions are comparable to those of cervids recorded in Middle to Late Pleistocene Indochinese sites (Khok Sung, Thum Prakai Phet, Duoi U'Oi) (Bacon et al., 2008a; Filoux et al., 2015; Suraprasit et al., 2016). *R. unicolor* is recorded in Chinese sites since the Early Pleistocene (Norton et al., 2010).

One fragmentary maxillae (CM125 with D3-D4-M1) and 158 teeth (NISP = 161) are assigned to *Muntiacus* sp. (P2s exhibit salient paracone and metastyle, and a marked fold between the hypocone and the protocone; buccal cusps and style are particularly salient on upper molars). The genus is common in southeast Asia and China since the Early Pleistocene (Tin Thein, 1974; de Vos and Long, 1993; Tougard, 1998; Bacon et al., 2008a, 2008b; 2011; Chen et al., 2002; Norton et al., 2010; Wang et al., 2014; Filoux et al., 2015) (SI-Table 1).

The eighty-three teeth of the large-sized bovid are massive with a thick enamel (Fig. 6, SI-Table 2). The p3s and p4s display well-developed V-shaped parastylid and paraconid (as salient as the metaconid). The postprotocristid and metaconid are particularly large, like in *Bos* species. Among the nine m3s, six have a salient entostylid forming a deep notch with the hypoconulid as also observed in *Bos*, and all have an anterior ectostylid. The cristid of the hypoconulid is particularly salient posteriorly, as in *Bos sauveli*. It seems that only one taxon was present at Coc Muoi, possibly *Bos sauveli* (kouprey). Dimensions show that molars are more massive than those of *B. sauveli* recorded at Tam Hang (Bacon et al., 2008b, 2011), and Khok Sung (Suraprasit et al., 2016). The species has not been recognized in south China (Rink et al., 2008; Wang et al., 2007, 2014).

Twenty-four teeth show the basic features of the serows (presence of styles and stylids more prominent than cusps, and smooth enamel). On some m3s, the metastylid and hypoconulid are particularly salient. Dimensions of teeth are close to those of *Capricornis sumatraensis* and C. *milneedwardsi*, than to those of *C. crispus*, *Naemorhedus caudatus,* and *N. goral* (Suraprasit et al., 2016) (SI-Table 2). The former species is also recorded at Wuyun in south China (Chen et al., 2002).

Suids are represented by 252 teeth and a jaw fragment (SI-Table 1). All teeth show the *Sus scrofa* pattern characterized by the presence of star-like folds and numerous accessory tubercles on the main cusps and cuspids of molars (observed on m3s and M3s) (Tougard, 1998; Suraprasit et al., 2016). The species is recorded in Middle to Late Pleistocene Indochinese (Bacon et al., 2008a, 2008b; 2012) and Chinese sites (Rink et al., 2008; Wang et al., 2007, 2014; Norton et al., 2010).

4.2.2. Perissodactyla

Three rhinocerotid taxa co-occur at Coc Muoi, all of them having close affinities with living Asian rhinoceroses. In terms of abundance, the Javan rhinoceros *Rhinoceros sondaicus* (NISP = 338) widely dominates over the Sumatran rhinoceros *Dicerorhinus sumatrensis* (NISP = 20) and a larger morph, referred to as *Rh. unicornis*, the Indian rhinoceros (NISP = 6) (Fig. 7).

Rhinoceros sondaicus is mostly documented by jugal teeth (D/d, P/p, and M/m), even if a small mandibular fragment is preserved as well as four i2s. Dental dimensions widely overlap those of recent representatives of *Rh. sondaicus* as provided by Guérin (1980) on permanent teeth (SI-Table 3), be that for small samples (upper teeth) or widely represented loci (lower teeth). Only the first upper premolars (persistent D1), M1s, and M2s have an anatomical length slightly exceeding the uppermost values for recent representatives of the Javan rhinoceros. Conversely, one m1 (CM1087) is unusually small (length = 32 mm; anterior width = 22 mm; posterior width = 23.5 mm). The material from Coc Muoi differs from that of Yanliang Cave (early Pleistocene, South China), assigned to

Table 1
Quartz OSL single-grain and feldspar pIR-IRSL single-aliquot dating of sediments from Coc Muoi cave.

Sample Code	Depth (m)	Grain Size (μm)	Beta dose rate[a] (Gy ka^{-1})	Field gamma dose rate[b] (Gy ka^{-1})	Cosmic-ray dose rate[c] (Gy ka^{-1})	Water content[d] (%)	Int dose rate (Gy ka^{-1})	Total dose rate[e] (Gy ka^{-1})	Technique[f]	Equivalent dose[g,h,i] (Gy)	Age[j] (ka)
COCMU 5	0.40	180–212	0.683 ± 0.024	0.254 ± 0.004	0.078	18/13 ± 5	0.032	1.047 ± 0.062	**UV**$_{SG\ OSL}$	122 ± 26	117 ± 27
	0.40	90–125	0.722 ± 0.026	0.254 ± 0.004	0.078	18/13 ± 5	0.840	1.774 ± 0.118	**pIR-**$_{SA\ IRSL}$	263 ± 11	148 ± 13
COCMU 6	1.00	180–212	0.683 ± 0.024	0.263 ± 0.024	0.078	18/13 ± 5	0.032	1.056 ± 0.062	**UV**$_{SG\ OSL}$	132 ± 25	125 ± 26
	1.00	90–125	0.722 ± 0.026	0.263 ± 0.024	0.078	18/13 ± 5	0.840	1.783 ± 0.119	**pIR-**$_{SA\ IRSL}$	260 ± 10	146 ± 12

[a] Beta dose rates determined from beta counter measurements of dried and powdered sediment samples. The dry dose rates calculated were adjusted to the water content.
[b] Determined from U, Th and K dose rates measured using a portable gamma-ray spectrometer at field water content.
[c] Time-averaged cosmic-ray dose rates (for dry samples), each assigned an uncertainty of ±10%.
[d] Field/time-averaged water contents, expressed as (mass of water/mass of dry sample) x 100. The latter values were used to calculate the total dose rates by using saturation tests on the raw dosimetry material.
[e] Mean ± total (1σ) uncertainty, calculated as the quadratic sum of the random and systematic uncertainties.
[f] Two luminescence technique were applied to these samples UVSG = quartz UV single-grain and p-IR-IRSL = post-infrared infrared stimulated luminescence dating of single-aliquots of feldspars.
[g] The Statistical model used to determine the De used for age calculation -MAM - Minimum Age Model.
[h] Palaeodoses include a ±2% systematic uncertainty associated with laboratory beta-source calibrations.
[i] UVSG measured using single-grains of quartz at least 1000 grains run for each sample, while pIR-IRSL incorporated 24 aliquots of a few hundred grains.
[j] Uncertainties at 68% confidence interval.

Table 2
Uranium-series dating of flowstone from Coc Muoi cave. Bold numbers are main results.

Sample Name	Sample depth[a]	U (ppm)	^{232}Th (ppb)	(^{230}Th/^{232}Th) ratio[b]	(^{230}Th/^{238}U) ratio	(^{234}U/^{238}U) ratio[b]	Uncorr. Age (ka)[b]	Corr. Age (ka)[b]	Corr. Initial (^{234}U/^{238}U)
VCOCMU-F3	60	0.14	92.41	5.19 ± 0.03	0.986 ± 0.004	1.3789 ± 0.001	126 ± 1	**114 ± 6**	1.62
VCOCMU-F4	75	0.15	35.43	6.08 ± 0.02	0.941 ± 0.003	1.3723 ± 0.002	118 ± 1	**108 ± 4**	1.58

[a] Measured from base of the cave floor to sampling height in cm.
[b] Uncertainties at 95% confidence interval.

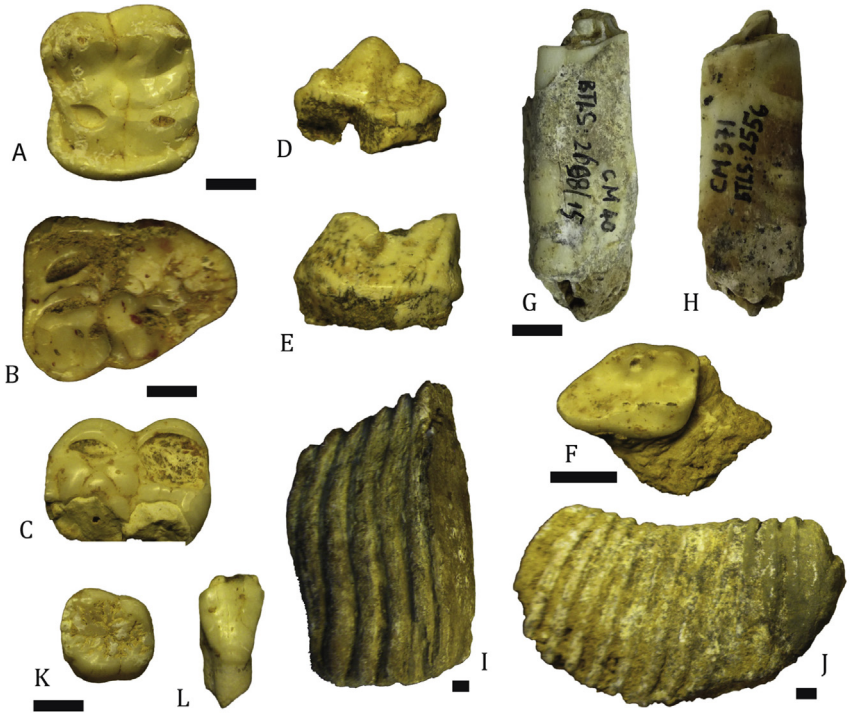

Fig. 6. Teeth from Coc Muoi cave. A-C, *Ailuropoda melanoleuca fovealis*. A, left upper M1 CM544 in occlusal view. B, right upper M2 CM546 in occlusal view. C, right lower m2 CM565 in occlusal view. D-E, *Panthera tigris*. D, left upper P3 CM534 in lingual view. E, left lower m1 CM632 in labial view. F, right upper M2 of *Helarctos* cf. *mayalanus* in occlusal view. G-H, large bovids. G, left lower m2 CM40 in distal view, with a marked hypoplastic groove on the basal third of the crown. H, one lobe of a fragmentary lower molar CM371 with two visible lines of discoloration of the enamel. I-J, *Elephas maximus*. I, fragmentary lower m2 CM730. J, right lower m1 CM734 in labial view. K-L, *Pongo* sp. K, left upper M1/M2 CM585 in occlusal view. L, right lower i1 CM625 in labial view. Scale bar = 10 mm.

Rhinoceros fusuiensis by Yan et al. (2014), in having a smooth metacone fold on upper premolars, a smoother paracone fold and a thicker hypocone on M1-2, a weak paracone fold on D1, a sharp parastyle on D2, a curved protoloph on D3, a more developed trigonid on p2, a rounded trigonid on lower cheek teeth, a posterior valley open lingually on d2, and a constricted metaconid on d3. All of these specimens have a consistent morphology, perfectly matching that of *Rh. sondaicus*, either recent (*e.g.* Guérin, 1980; Antoine, 2012) or Pleistocene in age (*e.g.* Hooijer, 1946; Colbert and Hooijer, 1953; Bacon et al., 2004, 2008b, 2011, 2015; Zeitoun et al., 2005). In particular, D1 has a teardrop-shaped occlusal outline. D1-2s display a smooth paracone fold. The mesostyle is posteriorly displaced on D2. D3 has a quadrangular occlusal outline and a curved protoloph. The protocone is not constricted on D4 and P3-4. D3-4s and M1-2s have no lingual groove on the hypocone. Enamel is wrinkled and arborescent on permanent cheek teeth. The external folds of P-M (paracone, mesostyle, and metacone) are vertical in labial view. The metacone fold is smooth on upper premolars. The hypocone and the protocone are equally developed on P4. Upper molars have no anterior constriction on the protocone. M1-2s have a curved protoloph. M3 is smaller than M1-2. The paralophid of d2 forms a bulbous spur. The anterior ectolophid groove is absent on d2 and marked on d3. In lingual view, posterior valleys are V-shaped on d3-4 and p2. The ectolophid groove is shallow on p2. The lingual side of the metaconid is convex in occlusal view at any wear stage on lower molars.

Six jugal teeth document a larger species, recognized as *Rhinoceros unicornis* (one M2, two M3s, one d2, one p4, and one m3) (Fig. 7). With no exception, these specimens exceed the dental size range of both *Rh. sondaicus* and *D. sumatrensis* and fall within the range of *Rh. unicornis* in terms of dimensions (SI-Table 4; Guérin, 1980) and morphological features. Enamel is wrinkled and corrugated, thick labially and thin on the lingual side of the ectolophs (M2: CM1105 and M3: CM1151). Cheek teeth are high-crowned and have neither lingual nor labial cingulum. The paracone fold vanishes toward the neck of M2. The protoloph is curved on M2. There is no lingual groove on the hypocone of M2. M3 seems not to be reduced in size with respect to M2. The hypocone is pinched on M3 (CM1151). The posterior valley is partly closed and the paralophid is bulbous and spur-like, which determines a deep anterior ectolophid groove on d2 (CM987). The metaconid of m3 has a convex lingual side in occlusal view (CM1033).

Dicerorhinus sumatrensis also occurs at Coc Muoi. It is represented by 20 upper and lower deciduous and permanent cheek teeth the dimensions of which mostly overlap those of *Rh. sondaicus*, notably from Coc Muoi (*e.g.* D1-4, P3, or M2-3; SI-Table 4). Such

Fig. 7. Rhinocerotid remains from Coc Muoi Cave. A-Q, *Rhinoceros sondaicus*. A, right D1 CM1108 in occlusal view. B, left D2 CM1042 in occlusal view. C, left D4 CM1132 in occlusal view. D, left P3 CM1046 in occlusal view. E, left M1 CM1104 in occlusal view. F, left M3 CM1106 in labial view. G-H, left d1 CM1017 in occlusal (G) and lingual views (H). I, left d2 in occlusal view. J, left d3 CM1326 in occlusal view. K, left d4 CM1028 in occlusal view. L, left p2 CM1058 in occlusal view. M, left p3 CM997 in occlusal view. N, left p4 CM1067 in occlusal view. O, left m1 CM1123 in occlusal view. P, left m2 CM1011 in occlusal view. Q, left m3 CM1010 in occlusal view. R-Y, *Rhinoceros unicornis*. R-S, right M3 CM1151 in labial (R) and occlusal views (S). T-U, left d2 CM987 in occlusal (T) and labial views (U). V-W, right p4 CM1094 in occlusal (V) and labial views (W). X-Y, right m3 CM1033 in occlusal (X) and labial views (Y). Z-I′, *Dicerorhinus sumatrensis*. Z, right D1 CM1289 in occlusal view. A′, left D2 CM1130 in occlusal view. B′, right D3 CM1143 in occlusal view. C′, right P4 CM1109 in occlusal view. D′, left M3 CM1107 in occlusal view. E′, left d2 CM1114 in occlusal view. F′, left d3 CM1208 in occlusal view. G′, right p4 CM1085 in occlusal view. H′-I′, left m3 CM1074 in occlusal (H′) and labial views (J′). Scale bar = 10 mm.

overlaps have precluded most taxonomic assignments at the genus/species level for isolated rhinocerotid teeth from Pleistocene-Holocene localities in Asia (*e.g.*, Hooijer, 1946). In fact, only the P4 (CM1109) and lower teeth (d3, p4, and m2-3) are smaller and narrower than those of *Rh. sondaicus* (SI-Table 4). Dimensions of P3-4 and of lower permanent cheek teeth fall within the range of *D. sumatrensis*, whereas the M2 (CM1133) and M3 (CM1107) are significantly larger than expected for the latter taxon (SI-Table 4). All these specimens were assigned to *D. sumatrensis* on morphological grounds, after direct comparison with unparalleled samples from Sumatran Pleistocene localities at Naturalis, Leiden (POA), and comparison with the early Pleistocene Liucheng Cave sample (only lower teeth; Tong and Guérin, 2009): D1 has a pentagonal occlusal outline. D1-2s display a strong paracone fold. The mesostyle is located on the anterior half of the ectoloph on D2. D3 has a trapezoidal occlusal outline and a sigmoid protoloph in occlusal view. There is a shallow protocone constriction on D4 and P3-4. D3-4s and M2s have a lingual groove on the hypocone. Enamel is corrugated on permanent cheek teeth. The external folds of P-M (paracone, mesostyle, and metacone) are oblique in labial view. The metacone fold is thick on P3-4. The hypocone is less developed than the protocone on P4 and upper molars. P4 and upper molars have a smooth anterior constriction on the protocone. M1-2s have a sigmoid protoloph. M3 has similar width and length as M1-2. The

paralophid of d2 is bifurcated. The anterior ectolophid groove is marked on d2 and absent on d3. In lingual view, the posterior valley is U-shaped on d3. The lingual side of the metaconid is flat in occlusal view on m2-3 (Fig. 7).

Two tapirids co-occur at Coc Muoi, with representatives of both the extant *Tapirus indicus* and the fossil Asian species *Megatapirus augustus* (Middle and Late Pleistocene; Tong, 2005) (Fig. 8; SI-Table 5). The dental remains of *T. indicus* (five permanent teeth, including a germ) and *M. augustus* (five permanent teeth) can easily be distinguished on the basis of size and morphology (Colbert and Hooijer, 1953). On the other hand, they seem not to overlap the intermediate dimensions of the Early and Middle Pleistocene *Tapirus sinensis* (SI-Table 5; Tong, 2005). Three more permanent tapirid teeth are not assignable at the specific or generic level. Among them, a lower canine (CM1077) is 17 mm wide and 13 mm high (crown height).

4.2.3. Proboscidea

Twenty-two teeth can be assigned to *Elephas* (five complete and nine incomplete teeth; seven isolated lamellae; one fragmentary tooth) (Fig. 6). Table 3 compiles the characteristics observed on the most easily determinable specimens. On the nearly complete m1 (CM734), the enamel wear pattern of the ridges 2 and 3 is tripartite, with loops coarsely and irregularly folded (Van den Bergh, 1999). One m2 (CM730) can be determined on the remaining six unworn lamellae vertically folded in a sinusoidal way, a h/w indice of 222, and a maximal width of 72.4 mm (Roth and Shoshani, 1988). Most characteristics point to the presence of *E. maximus* instead of *E. namadicus*: the number of lamellae (for d2, five in the Coc Muoi species *versus* three in *E. namadicus*; for d3, 9 *vs* 5–7; for D3, 9 *vs* 6–7; for m1, 14–17 *vs* 9–11; for m2, 16–21 *vs* 11–15); the overall dimensions of teeth and the h/w index (for m2, 222 vs 180–188) (Maglio, 1973; Roth and Shoshani, 1988). We do not observe any worn enamel figures with pointed median expansions (Maglio, 1973). The presence of *E. maximus* is also reported in southern China possibly since 300 ka (Wuyun and Tantang sites) (Chen et al., 2002; Wang et al., 2007, 2014; Li et al., 2017).

Despite their highly fragmentary state, six specimens clearly belong to *Stegodon* sp. The isolated lophs are ridge-shaped with dimensions that indicate low crowns. The width of enamel is comprised between 4.4 mm and 5.9 mm (Van den Bergh, 1999; Colbert and Hooijer, 1953).

4.2.4. Carnivora, primates and rodentia

Five teeth conform to the dental pattern of the canid *Cuon alpinus*. The anterior width of one P4 falls within the range of the Duoi U'Oi teeth (Bacon et al., 2008a). The assignment of the Coc Muoi specimens to *C. alpinus antiquus* is not supported, contrary to those from Middle to Late Pleistocene sites, Tam Hang, Wuyun and other Chinese sites (Colbert and Hooijer, 1953; Chen et al., 2002; Wang et al., 2007; Norton et al., 2010; Bacon et al., 2011).

Two small felids (NISP = 7) have the same morphology but a different size (SI-Table 6). Five jugal teeth and one canine conform to the morphology and size of *Panthera tigris* (SI-Table 7). This identification remains questioned for one p3 which falls within the inferior limit of the range size of p3 in modern tigers. All teeth are massive, particularly one P4. The tiger is recorded in China since the transition between the Early and the Middle Pleistocene (Norton et al., 2010).

Eleven teeth of melines suggest the presence of two taxa. Two M1 have a relatively small size, whereas another one is much longer (16.6 mm *vs* 20.1 mm). One P4 is as long as those of *Arctonyx collaris rostratus* described at Yenchingkuo (Colbert and Hooijer, 1953).

One fragmentary P4 is attributed to the mustelid *Martes* sp., thanks to the morphology of the anterior cusplet well-developed on the lingual side. One worn m1 of a viverrid is identified as *Paradoxurus* sp. (SI-Table 6). The main cuspids are low with a globular shape. The talonid has few developed cuspids, and a rounded outline. But contrary to *P. hermaphroditus* also recognized at Tam Hang (Bacon et al., 2011), the paraconid of the Coc Muoi tooth is particularly well-individualized. The genus *Paradoxurus* is known in southeast Asia since the Middle Pleistocene, whereas that of *Martes* is present in China since the Early Pleistocene (Norton et al., 2010).

Most of the twenty jugal teeth have the size and morphology of *Ursus thibetanus*, whereas only two molars could belong to *Helarctos malayanus* (the m1 is not elongated mesiodistally and the talonid is not separated by a large notch from the trigonid, as in *U. thibetanus*; the M2 is more square). Eleven canines are left in open nomenclature (*Ursus* sp.). Dimensions of both taxa match those of Duoi U'Oi and Tam Hang (Bacon et al., 2008a, 2008b, 2011). The Chinese specimens assigned to *U. thibetanus kokeni* are slightly larger (Colbert and Hooijer, 1953) (SI-Tables 9-10).

Nine jugal teeth have dimensions closer to those of the Middle Pleistocene *Ailuropoda melanoleuca fovealis* from China than to the

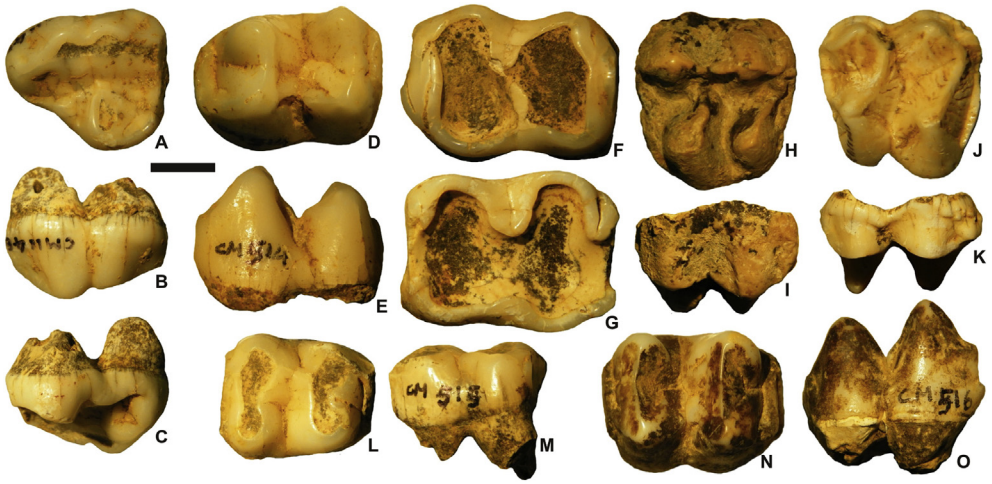

Fig. 8. Tapirids from Coc Muoi cave. *Megatapirus augustus*. A-C, left P1 CM1146 in occlusal (A), labial (B) and lingual views (C). D-E, left p3 CM514 in occlusal (D) and labial views (E). F, left m1 CM1145 in occlusal view. G, right m1 CM1144 in occlusal view. *Tapirus indicus*. H-I, right P2 CM1040 in occlusal (H) and labial views (I). J-K, right M1/2 CM1147 in occlusal (J) and labial views (K). L-M, left p3 CM515 in occlusal (L) and labial views (M). N-O, left p4 CM516 in occlusal (N) and lingual views (O). Scale bar = 10 mm.

Table 3
Characteristics of the Coc Muoi teeth assigned to *Elephas maximus*. Cheek teeth dimensions; number of lamellae (P); Width of enamel; Frequency of lamellae (number of lamellae on 10 cm along the longitudinal plan of the tooth); Index of hypsodonty (H x 100/W); Number of worn lamellae on the grinding occlusal surface (Maglio, 1973; Roth and Shoshani, 1988; Van den Bergh, 1999). The age of individual is estimated using the number of worn lamellae on the grinding surfaces of lower teeth, and age reference chart based on specimens of *E. maximus* of known age (Roth and Shoshani, 1988: Fig. 7). J. Juvenile; SA, Subadult; A, adult.

	type	Length (mm)	Width (mm)	Height (mm)	P	Width of enamel (mm)	Frequency of lamellae	Hx100/W	Number of worn lamellae	Estimation of age
CM721	D3	68.1	35.5 (lame 6)	52	9	–	–	146.4	3	–
CM735	rD3	67.1	31.6 (lame 3)	54.6	9	–	–	172.7	3	–
CM727	rd2	20.8	12.9 (lame 4)	12.1	5	–	–	–	5	1 yr (J)
CM722	rd3	75.5	35.8 (lame 7)	52.6	9	–	–	146.9	4	1-4 yrs (J)
CM723	d3	–	24.8	34.6	1+	–	–	–	–	–
CM724	d3	–	28.1	28.7	1+	–	–	–	–	–
CM736	d3	–	23.9	25.4	1+	–	–	–	–	–
CM737	d3	–	22.1	32.9	3+	–	–	–	–	–
CM738	d3	–	31	46.9	3+	–	–	–	–	–
CM739	d3	–	39.5	61.4	6+	–	–	155.4	<6	3-5 yrs (J)
CM725	d3/D3	–	–	–	1+	–	–	–	–	–
CM742	d/D	–	–	–	–	–	–	–	–	–
CM895	d3/D3	–	~40	41.3	1+	–	–	–	–	–
CM734	rm1	174.5	54.8 (lame 8)	98	14+	–	13	178.8	5	6-15 yrs (SA)
CM420	m1	–	–	>100.7	1+	3.68	–	–	–	–
CM733	m1	–	52.4	–	4+	–	–	–	–	–
CM729	m1	–	55.7	110.9	4+	–	–	199.1	<10-13	9-16 yrs (SA)
CM731	m1	–	60.9	>130.6	3+	–	–	–	–	–
CM732	m1	–	56.8	127.5	2+	–	–	–	–	–
CM730	m2	–	72.4	160.8	6+	–	–	222	<10-15	19-22 yrs (A)
CM728	m1/M1	–	50.6	>80	2+	–	–	–	–	–
CM741	m/M	–	–	–	1+	–	–	–	–	–

modern specimens (Colbert and Hooijer, 1953; Chen et al., 2013), with particularly one massive P4 (SI-Table 11).

Coc Muoi also records orangutans (NISP = 25), with dimensions close to those of the specimens referred to *Pongo devosi* (*i. e.* intermediate in size between Early to Middle Pleistocene *P. weidenreichi* from south China and Vietnam and modern species from Sumatra and Borneo) (Hooijer, 1948; Cuong, 1985; Olsen and Ciochon, 1990; Schwartz et al., 1994, 1995; Wang et al., 2014; Harrison et al., 2014) (SI-Table 12).

The set of teeth assigned to *Macaca* sp. (NISP = 23) and to a colobine indet. (NISP = 13), is composed of numerous heavily worn molars, that impedes assignment at a species level. Nevertheless, dimensions of m3 and M3 fall within the range of modern *M. mulatta* and *M. nemestrina* (Takai et al., 2014). One tooth of *Hylobates* sp. is identified. Seventy-nine teeth conform to the morphology pattern of porcupines *Hystrix* sp. and *Atherurus* sp. All taxa are recorded in Table 4.

4.3. Taphonomy

4.3.1. Gnawing traces and breakage on roots

The majority of the damage observed are breakage on crowns and roots, and gnawed marks on roots. The gnawing frequency in the assemblage is high (~82.5%) (SI-Table 13). The chisel marks are large and consistent with gnawing by porcupines. A significant part of the teeth belonging to Carnivora and Primates displays intact and ungnawed roots (9–40%). Differently, ungulates display ~84–100% of gnawed roots (in the large bovid sample particularly, ~85% of the teeth have roots totally gnawed).

Within the Coc Muoi ungulate sample, damage observed on rhinocerotid teeth show a particular pattern (Table 5). Whatever the type of the tooth (either permanent, milk, upper, or lower) a small percentage of teeth is intact (mean = 2.7% with values ranging from 1.3 to 3.5%). If most of the permanent teeth show a high proportion of gnawed roots (~84%) and a low proportion of broken roots (a part of them further showing no gnawing evidence; 13.7%), milk teeth are either gnawed or broken in similar extents (49.3% and 47.2%, respectively; no difference between upper and lower teeth). In other words, the proportion of teeth with gnawed roots is significantly higher for permanent teeth than for milk teeth (Khi-2 = 8.54; $p < 0.01$), whereas the percentage of broken roots is considerably higher for milk teeth than for permanent teeth (Khi-2 = 17.33; $p < 0.001$).

Eleven out of 13 tapirid teeth are gnawed (84.6%), apparently regardless of the individual age or the taxonomic assignment (SI-Table 13).

4.3.2. Frequency of upper vs lower, and permanent vs deciduous teeth

The data demonstrate a better survivorship of lower than upper teeth in large-sized ungulates (statistically significant for *Rh. sondaicus*; Khi-2 = 31.38; $p < 0.001$), and conversely a better survivorship of upper teeth in *Muntiacus*. Only *S. scrofa* shows upper teeth almost as preserved as lower teeth. Most of the ungulate species are represented by more permanent than deciduous teeth no overabundance of milk teeth in *Rh. sondaicus* (Khi-2 = 3.72; $p > 0.05$), except for *D. sumatrensis* with teeth in equal number, and proboscideans with more deciduous than permanent teeth (Table 4, and Supplementary Information).

All types of lower teeth (incisor, canine, premolar, and molar) are preserved for *R. unicolor*, and it is likely that among the remains of carcasses deposited at the site, there were some complete mandibles. Pig data allow us to speculate that some complete jaws were most probably deposited. Regarding perissodactyls, virtually no associated elements were recognized, except for one pair of d4 referred to as *Rh. sondaicus* [CM1118 and CM1253], which would point to significant post-mortem dismemberment for the entire sample.

Fig. 9 illustrates the compilation of values for both indexes (NISP and MNIf) by species for all teeth examined (upper/lower/permanent/deciduous). It clearly shows the great abundance of all ungulate species, and particularly that of *Rh. sondaicus*. Despite the differences in the frequency of teeth, NISP produce comparable abundance (MNIf) for *B.* cf. *sauveli*, *R. unicolor*, and *S. scrofa*.

Table 4
Taxa identified in the Coc Muoi assemblage. NISP: Number of identified specimens; MNIf: Minimum number of individuals (frequency); MNIc (combination). The assemblage is composed of 1316 isolated teeth, four fragmentary jaws (*R. unicolor*, *Sus scrofa*, and *Muntiacus* sp.), and one edentulous fragment of a corpus mandibulae of an unidentified rhinocerotid (NISP = 1323). *Rhinoceros sondaicus* MNIc equals 54: at least 32 juveniles (19 ld4 + 14 rd4 including one left-right pair clearly identified: CM1118-CM1253), and 22 adult individuals (22 functional rm3 incompatible with d4s within a single individual). By contrast, *Rh. unicornis* MNIc includes two adults and one juvenile (two functional rM3s + one d2, incompatible with M3s within a single individual), and that of *D. sumatrensis* coincides with three adults and three juveniles (three non-paired functional m3s + three non-paired D2s, further incompatible with M3s). (J) juvenile; (SA) subadult; (YA) young adult; (PA) prime (mature) adult; (OA) old Adult; (A) adult. A few teeth of adult *Stegodon* recovered during previous survey are not included.

Species	NISP	Permanent teeth			Deciduous teeth			MNIf	MNIc
		upper	lower	u/l	upper	lower	u/l	–	–
Rusa unicolor	152	47	86	–	4	15	–	12A, 5J	–
Medium-sized cervid	16	5	8	–	–	3	–	2A, 2J	–
Bovid/Cervid	11	5	5	1	–	–	–	–	–
Muntiacus sp.	161	103	44	–	12	2	–	5A, 6J	–
Bos cf. *sauveli*	83	12	67	–	4	–	–	14A, 4J	–
Capricornis sp.	24	12	12	–	–	–	–	3A	–
Sus scrofa	252	121	113	5	6	2	5	15A, 3J	–
Megatapirus augustus	5	1	4	–	–	–	–	2A	1J, 1SA, 4A
Tapirus indicus	5	2	3	–	–	–	–	2A	
Tapiridae indet.	3	1	2	–	–	–	–	1A	–
Rhinoceros sondaicus	343	65	145	–	53	80	–	19A, 19J	33J, 22A
Rhinoceros cf. *unicornis*	6	3	2	–	–	1	–	2A, 1J	1J, 2A
Dicerorhinus sumatrensis	20	4	6	–	–	10	–	2A, 2J	3J, 3A
Rhinocerotidae indet.	1	–	1	–	–	–	–	–	–
Elephas maximus	22	–	7	2	2	8	3	3A, 2J	3J, 2SA, 1A
Stegodon sp.	6	–	–	2	–	–	4	1A, 1J	–
Cuon alpinus	5	2	2	1	–	–	–	1A	1YA, 1MA
Martes sp.	1	1	–	–	–	–	–	1A	–
Paradoxurus sp.	1	–	1	–	–	–	–	1A	–
Large-sized meline indet. 1	4	3	1	–	–	–	–	2A	–
Small-sized meline indet. 2	7	3	2	2	–	–	–	2A	–
Small-sized felid indet. 1	4	3	1	–	–	–	–	2A	–
Small-sized felid indet. 2	3	1	–	2	–	–	–	1A	–
Panthera tigris	7	3	3	1	–	–	–	2A	1YA, 1MA, 1OA
Helarctos cf. *malayanus*	3	1	2	–	–	–	–	1A	2J, 2PA, 2OA
Ursus thibetanus	17	13	4	–	–	–	–	3A	
Ursus sp.	11	–	–	11	–	–	–	3A	–
Ailuropoda melanoleuca fovealis	9	5	4	–	–	–	–	2A	1YA, 1MA, 1OA
Pongo sp.	25	16	8	1	–	–	–	2A	–
Macaca sp.	23	10	12	1	–	–	–	3A	–
Colobine indet.	13	11	1	1	–	–	–	2A	–
Hylobates sp.	1	1	–	–	–	–	–	1A	–
Hystrix sp.	73	5	7	61	–	–	–	6A	–
Atherurus sp.	6	–	–	1	–	–	–	2A	–
Total	1323	460	552	92	81	121	12	165	

Table 5
Damage (gnawed root, broken root, or intact) and percentages observed on jugal teeth referable to rhinocerotids from Coc Muoi cave (upper/lower; permanent/deciduous).

	Total number	gnawed (%)	broken roots (%)	intact (%)
Upper and lower teeth	370	260/370 = 70.27	100/370 = 27.03	10/370 = 2.70
Upper teeth	130/370 (35.14%)	85/130 = 65.38	42/130 = 32.31	3/130 = 2.31
Lower teeth	240/370 (64.86%)	175/240 = 72.92	58/240 = 24.17	7/240 = 2.91
Permanent teeth (upper)	72/226 (31.86%)	59/72 = 81.94	12/72 = 16.67	1/72 = 1.39
Permanent teeth (lower)	154/226 (68.14%)	131/154 = 85.06	19/154 = 12.34	4/154 = 2.60
Deciduous teeth (upper)	60/144 (41.67%)	28/60 = 46.67	30/60 = 50	2/60 = 3.33
Deciduous teeth (lower)	84/144 (58.33%)	43/84 = 51.19	38/84 = 45.24	3/84 = 3.57

4.4. Age-at-death distribution and health status of large-sized species

4.4.1. Age-at-death distribution

In the *Rusa unicolor* profile (Fig. 10), all classes are represented, except those which contain very old individuals [9–10]. The adult category is composed of prime-aged and first old-aged individuals [3–7] equally represented, that corresponds to individuals weighting up to 260 kg (Francis, 2008). The Coc Muoi three-cohort pattern (18.5% of juveniles, 3.7% of yearling and 77.8% of adult individuals) matches with the profile of a living Indian population (Biswas and Sankar, 2002).

The *Bos* cf. *sauveli* profile contains all classes, from juveniles [1–2] to very old individuals [9–10] (Fig. 9). Three periods were particularly critical for the species: the juveniles [1], the youngest late prime adults [6], and the youngest old adults [9], giving a curve with three peaks. When compared the three-cohort profile (18.2% of young, 9.1% of juveniles and 72.7% of adult individuals) with demographic pattern of the gaur, no selection of age class can be emphasized (Karanth and Sunquist, 1995; Biswas and Sankar, 2002).

The Coc Muoi mortality pattern of *S. scrofa* shows the low representation of piglets [T-C] (Fig. 10). Considering the litter size of the species (up to 10 piglets when ecological conditions are favorable), the underrepresentation is most likely due to their rapid destruction. Mature adult individuals (up to 200 kg) are well-

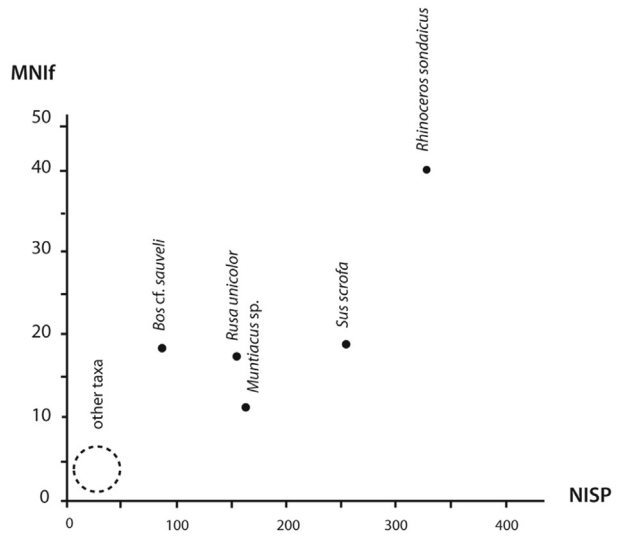

Fig. 9. Diagram with NISP on abscissa and MNIf on ordinate by species of the Coc Muoi fauna.

represented [G-J] whereas old-aged individuals are lacking [M-N]. The three-cohort model is nevertheless comparable to the demographic data of living populations (Karanth and Sunquist, 1995; Biswas and Sankar, 2002).

Mortality curves of rhinocerotids (including *Rhinoceros* and *Dicerorhinus* species) show three peaks, coinciding with juveniles [cohort IV: 12–18 months], subadults [cohorts VIII: 4–7 years], and adults [cohorts IX–XVI: 7–40 years] (Fig. 11A). The corresponding mortality curve is not significantly distinct from that of the structure of a recent natural population of *Rh. unicornis* (Chitwan Park; Laurie et al., 1983), as demonstrated statistically (Fig. 11). Our results do not demonstrate overrepresentation of age classes in any of the profiles.

Mortality patterns of the Coc Muoi species resemble attritional patterns with deaths most likely caused by multiple biotic and abiotic factors (diseases, starving, climate, and predation). All ungulate species enter the prey size category of the tiger (180–254 kg; Francis, 2008). Indeed, depending on their abundance locally, either chital, sambar deer, pig or gaur (Karanth and Sunquist, 1995; Bagchi et al., 2003; Andheria et al., 2007; Hayward et al., 2012) can be the preferred prey of tigers, even the most aggressive male pigs up to 200 kg, or the heaviest male gaur up to 1500 kg. It has been observed particularly that the behavior of solitary adult pig and sambar males may increase their encounter rate with the predator (Schaller, 1967; Johnsingh, 1992; Karanth and Sunquist, 1995; Leslie, 2011).

In relation to the kouprey and rhinoceroses, the "multimodal" curves suggest that deaths might have occurred during major biological, physiological, and behavioral events, and accordingly affect age classes of vulnerable individuals. In relation to large bovids, beside periods of immaturity [cohort 1] and old age [9], that of late prime adult age which corresponds to adult individuals over 10 years [6], represents a period of great vulnerability, when males leave "mixed breeding herds, to smaller, bachelors herds or more isolated existence" (Nowak, 1999; Bunn and Pickering, 2010). In its natural habitat, the solitary kouprey is more subject to predation by tigers, since it does not have the rest of the herd to help keep watch (Lekagul and McNeely, 1977). In relation to rhinoceroses, peaks also correspond to period of great vulnerability: weaning period [cohort IV], sexual maturity which occurs between 4 and 7 years depending on the gender [VIII], and solitary behavior for bulls more than 20 years old [XIII] (Laurie et al., 1983). The role of the tiger as main predator of these large prey is plausible, according to their availability (particularly juvenile rhinoceroses taking into account their abundance at the site) and chance encounter, but it remains tentative at that point.

4.4.2. Enamel hypoplasia

A high percentage of rhinocerotid teeth from Coc Muoi (71/264: 26.8%) show environmental enamel hypoplasia (EEH), thus expressing a severe physiological stress during odontogenesis, without a genetic origin (Mead, 1999). The frequency of rhinocerotid milk molars affected by EEH is very low (2.7%: 4/144; range: 0–6.06%), with only one D4, one d3, and two d4 expressing such pathology (SI-Table 17). Contrastingly, more than 30% of permanent teeth show signs of EEH, with percentages ranging from 0 (P2: 0/3) up to 47.3% (M3: 9/19). The frequency of loci affected by EEH equals or exceeds one third, 33.3% for m2, 35% for p4, 40% for P4 and m3, up to 44.4% for P3. Enamel hypoplasia is most expressed on the last premolars (P4 and p4; 11/30 = 36.6%) and molars (M3 and m3; 27/64 = 42.1%), *i.e.* the last functional teeth of the series (erupting at ~7–9 years in *Ceratotherium simum*; Hillman-Smith et al., 1986). The teeth affected show linear defects (43 teeth), enamel pits (28 teeth), less severe defects coinciding with horizontal striae (18 teeth), or a two-colored enamel (d1 CM1015). Fifteen teeth show both linear defects and enamel pits. Interestingly, 41 teeth are affected by multiphased EEH, with two (20 teeth), three (10 teeth), four phases (one tooth), or permanent defects (10 lower permanent teeth, all assigned to *Rh. sondaicus*). One-phased EEH is more frequent on the ectoloph (id) and it occurs mostly at the base of the crowns (late stage for odontogenesis), except for the d4 CM1413 (top of the crown).

Physiological stress responsible for EEH in rhinocerotids from Coc Muoi mostly occurred during odontogenesis of permanent teeth and as such it might point to severe post-natal undernutrition among the available sample during an individual age interval mostly encompassing weaning (at around 1.5 year) and abandonment (at around 3 years).

No trace of enamel hypoplasia is observed on tapirs. Regardless of the sample size, severe stigmata are essentially observed in *Rh. sondaicus*, probably indicating critical intraspecific competition for food resource in this taxon.

The percentage of examined kouprey teeth displaying enamel hypoplasia reaches 15.9% (10/69), a pathology only observed on permanent molars, 6.6% for m1 (1/15), 31.2% for m2 (4/16), and 55.5% for m3 (5/9), but unlike rhinocerotids, the data are biased due to the small number of milk teeth (SI-Table 18). For most of the teeth (9/10), the defects are horizontal furrow-form lines located on the basal third of crowns. On four teeth particularly (two m2 and two m3), the furrows are ~2 mm wide, deep and well-marked on both buccal and lingual sides of the crowns. Another molar displays a non-linear line of small pits.

Assessment of individual ages at defect formation is difficult, the literature outlining the considerable variation in the formation and eruption sequences of teeth in domestic animals, whereas those of wild animals are unknown. Globally, in large bovines, the complete formation of crowns achieves around 0.5 years for m1 (one third of crown already formed at birth), one year for m2, and two years for m3 (Hillson, 2005), pointing for the Coc Muoi population to a physiological stress after birth, during the juvenile period. According to the analysis of Niven et al. (2004) in bison dentition of two ancient populations, comparable stresses observed on m1s formed several weeks just after birth, most likely as a result of

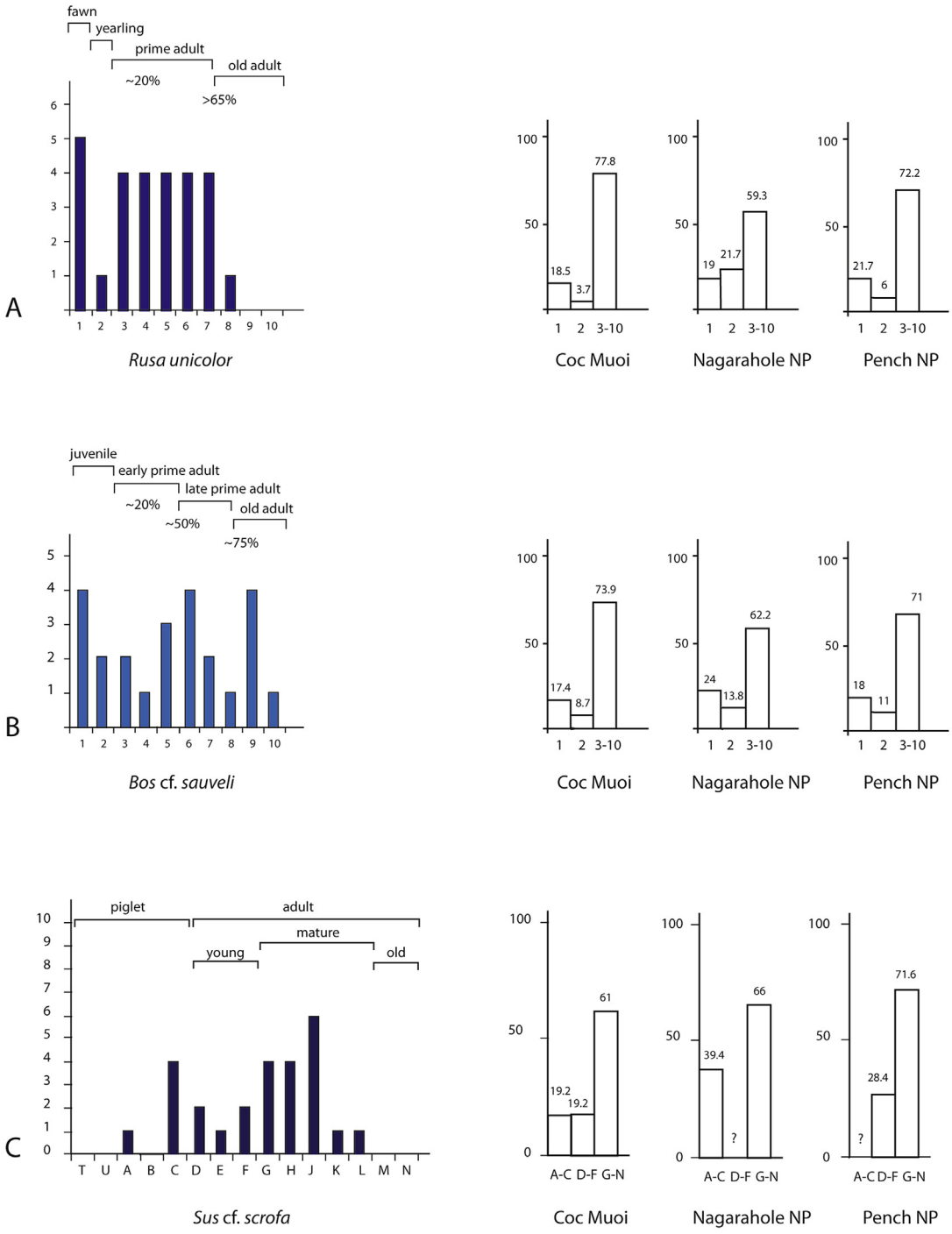

Fig. 10. Mortality profiles of (A) *Rusa unicolor*, (B) *Bos* cf. *sauveli* and (C) *Sus scrofa* from Coc Muoi cave. We used for comparison demographic data compiled in three-cohort patterns (juvenile, subadult, adult) from living prey-rich communities in India supporting the highest prey biomass densities (~6000 kg/km^2 for Pench Park and ~7600 kg/km^2 for Nagarahole National Park) (Karanth and Sunquist, 1995; Biswas and Sankar, 2002).

postnatal adjustment, and that on m2s can be associated to the dietary shift when calves wean at approximately nine months. Defects recorded on m3s all located at the same level on the crown could correspond to the age when individuals reach sexual maturity, slightly before and around two years, and then could represent physiological stress related to this activity as observed in other large mammals (Dobney, 2000). Nevertheless, the fact that the defects on teeth in some individuals are deep furrows visible on the circumference of crowns (4/11) suggest that they were caused by a combination of factors (such as diseases or seasonal changes in environmental conditions in addition to age-specific stressors) (Goodman and Rose, 1990). One isolated lobe of a lower molar displays two linear marks of discoloration of the enamel on the buccal side, also ~2 mm wide, one on the occlusal third and one on the basal third of the crown, which were most likely due to different causes (Fig. 6H).

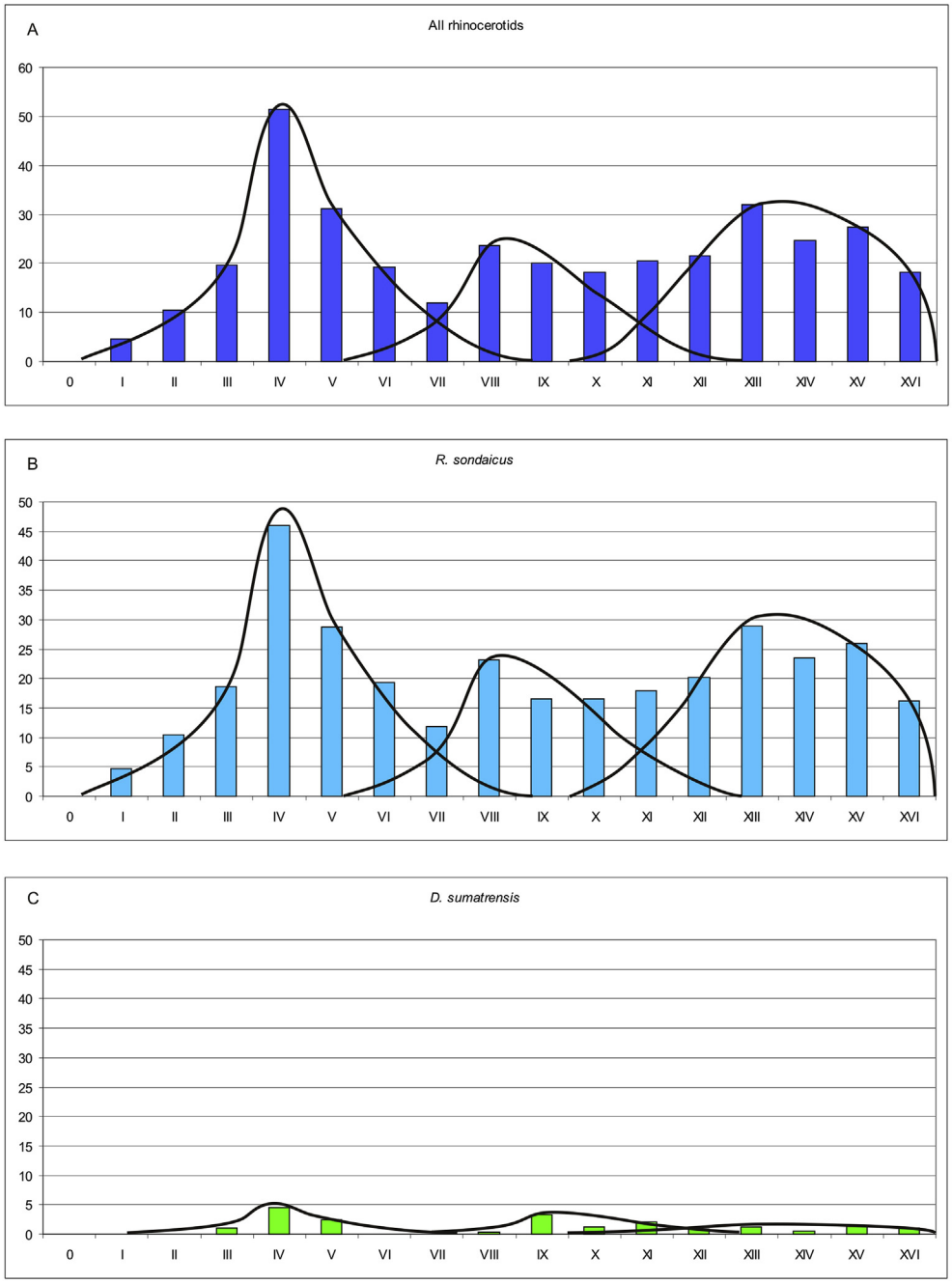

Fig. 11. Mortality curves of rhinocerotids from Coc Muoi cave, using the age classes of Hillman-Smith et al. (1986) and following the protocol of Bacon et al. (2008a, 2015). A. All rhinocerotids. B. *Rhinoceros sondaicus*. C. *Dicerorhinus sumatrensis*. Cohorts on abscissa and MNIc on ordinate.

5. Discussion

5.1. Age of the fauna

Considering the time frame for fossiliferous breccia deposition between 148 and 117 ka, the analysis of the Coc Muoi fauna provides information on terrestrial ecosystems in the northern part of the Indochinese region during MIS6-5. This period of deposition encompasses ~20 kyr of the later section of glacial stage MIS6 (186-128 ka), through the transition to the onset of the interglacial event MIS5 including the Eemian (MIS5e: 124-119ka).

The dating results indicate that the quartz SG-OSL dating provides the youngest age range for the deposit (125-117 ka), while the pIR-IRSL of feldspars is slightly older (148-146 ka) but still coeval within error limits. The additional feldspar analysis was conducted to ensure that the low acceptance of the single-grains of quartz had not skewed the final result, but the agreement between the two techniques on different minerals confirms the integrity and reliability of the SG-OSL result. The slight difference in age ranges between the techniques represents the different bleaching properties of the minerals; the quartz OSL signal bleaches more rapidly than the high temperature feldspar signal used for pIR-IRSL techniques. The bleaching properties of the feldspar signal were tested during the pIR-IRSL procedure (see Supplementary Information) and revealed a residual dose of ~12 Gy and this value formed the basis of the residual correction of the final equivalent dose (D_e)

value. However, there is a strong likelihood that the feldspar grains were partially bleached before entering the cave. In comparison, the quartz grains that showed the least amount of partial bleaching were isolated in the SG-minimum age model and have strongly influence the final age. Thus, the difference between the use of the SG *vs* SA techniques and quartz *vs* feldspar minerals account for the slight difference in age between the techniques. However, the age range obtained from both techniques is older than the age of the overlying flowstone (114-108 ka) suggesting integrity in sediment deposition and later flowstone capping.

This proposed age range (148-117 ka) agrees with the biochronological context presented by the associated Coc Muoi faunal assemblage. Indeed, the fauna is strongly reminiscent of other mammalian faunas known to postdate ~300 ka in Southeast Asia and south China. Noteworthy is the absence of any Neogene taxa characteristic of the Early Pleistocene (2.6–0.8 Ma) (Wang et al., 2007, 2014; Rink et al., 2008; Norton et al., 2010; Jin et al., 2014). The association between modern species (>41% considering the identified species) and archaic taxa (*Stegodon orientalis* and *Megatapirus augustus*) is common in the Middle to Late Pleistocene of the region (Wang et al., 2007; Rink et al., 2008). Such assemblages document the "*Stegodon-Ailuropoda* faunal complex", likely surviving until the Pleistocene–Holocene transition (Turvey et al., 2013). Furthermore, the absence at Coc Muoi of *Pachycrocuta brevirostris* and *Gigantopithecus blacki* recorded at Tham Khuyen in the Lang Son province (~475 ka; Ciochon et al., 1996), would also support a younger age. Indeed, the extinction of the giant ape is now estimated to have occurred around 300 ka (Wang et al., 2007; Rink et al., 2008; Zhang et al., 2014; Bocherens et al., 2017). It may be added that the Coc Muoi-type fauna persisted in south and central China until the arrival of first *Homo sapiens* as suggested for the moment by the faunal composition of the Liujiang (>280-87 ka; Shen et al., 2002), Huanglong (100-80 ka; Liu et al., 2010a), Zhiren (116-106 ka, Liu et al., 2010b; Cai et al., 2017), Luna (126.9–70.2 ka; Bae et al., 2014), and Fuyan sites (120-80 ka; Liu et al., 2015).

5.2. Review of pre- and postdepositional factors

The data confirm the significant role of porcupines (*Hystrix brachyura*, 15–20 kg; Francis, 2008) as the last agents to accumulate and modify the bones at the site before burial (Pei, 1935; Lenoble et al., 2006; Storm and de Vos, 2006; Tong et al., 2008). As already noticed for other Asian sites (Bacon et al., 2015), ungulates were the preference of porcupines for their gnawing activities (~84–100%). In this respect, the Coc Muoi data are comparable to those of Duoi U'Oi (70-60 ka; Vietnam) and Sibrambang (80-60 ka; Sumatra), and differ to those of Tam Hang (98-60 ka; Laos), and Nam Lot (86-72 ka; Laos) in which all groups (ungulates, carnivora and primates) are indistinctly concerned by damage inflicted by porcupines.

The possible causes of this differential treatment of remains by large rodents are to be found in the ecological context within each site. Porcupines collect available and transportable remains of carcasses of animals killed or scavenged by predators. This collect most likely depends on the availability of carcasses and state of preservation in which predators let the prey consumed (Duoi U'Oi, Sibrambang and Coc Muoi are tiger sites, whereas Tam Hang and Nam Lot were dominated by group-living voracious dholes and hyenas). Additional factors involved in the selection of remains by porcupines might be weight, size, density of elements (Brain, 1981), and the fact that in certain species, mandibles can be easily detachable from skulls (deer, cattle, and rhinoceroses), or not (pig), as suggest taphonomic clues.

Somewhat distinct post-mortem histories can be assumed however for the rhinocerotid sample at Coc Muoi: porcupines might have played a more prominent role for transporting and/or accumulating permanent teeth than milk teeth, whereas another external factor, such as post-mortem destruction by water flows or carnivores, might have been responsible of damage inflicted on milk teeth, more fragile.

In relation to postdepositional (postburial) factors, the transportation by water inside the karsts most likely resulted in an additional selection of teeth, those of middle to large-sized mammals with respect to small mammals (Duringer et al., 2012).

5.3. Reconstruction of the environmental context

5.3.1. Assessment of the Coc Muoi palaeoecological context

At latitudes close to that of Coc Muoi (22° N), sedimentological and palynological records of the Leizhou Peninsula (20°–21° N) in southern China show that a continuous rain forest cover remained throughout the glacial period MIS6 with relatively cool and wet conditions (temperatures were estimated to be more than 4 °C lower than present), followed by a warmer climate with a vegetation dominated by monsoon evergreen forests (MIS5 marked by a strong rise of *Catanopsis* and *Quercus* species) (Zheng and Lei, 1999).

It becomes clear that the Middle to Late Pleistocene ecosystems which occurred at these latitudes in Southeast Asia (23°-20°N) have no equivalent with any current ecosystems in Asia. The Coc Muoi forested habitat type supported a high ungulate biomass, a total of eight herbivore taxa weighing 250 kg up to 5000 kg (SI-Table 23). The most abundant ungulates <250 kg (sambar and pig) are known to be forest-dwelling species, but with a broad ecological flexibility, and they likely feed also in more open areas (Schaller, 1967; Nowak, 1999; Leslie, 2011; Ramesh et al., 2012).

A recent stable isotopic analysis of cervid teeth ($\delta^{18}O$ and $\delta^{13}C$) from Tantang cave in Guangxi, estimated late Middle Pleistocene in age on the basis of the faunal composition comparable to those of Wuyun (300-70 ka), suggests that cervids lived in a canopied woodland. Results also suggest that they might have fed in more open areas at the site (Li et al., 2017). Results based on $\delta^{18}O$ values range show that the period was impacted by strong summer monsoons. In another analysis, isotopic results of Pleistocene taxa from the Guangxi area (but with unclear dating), show that the giant panda, stegodon, rhinoceros, bovids and cervids all relied on C_3-based food from canopied woodlands (Bocherens et al., 2017), and likewise the Late Pleistocene elephant from the region (Ma et al., 2017).

The presence of the tiger at Coc Muoi strongly supports the presence of a diversified habitat with closed forests and zones with more open forests (Schaller, 1967).

5.3.2. Specificities of the Coc Muoi rhinocerotid sample

Specific attention has been centered on Coc Muoi rhinoceroses given their exceptional abundance and distribution of individuals among age classes. When considered the data in three-cohort patterns, the distribution of the Coc Muoi rhinocerotids (including *Rhinoceros* and *Dicerorhinus*) and, to a lesser extent that of Duoi U'Oi (70-60 ka, northern Vietnam; Bacon et al., 2008a, 2015), coincide with that of a natural population with no apparent bias related to either predation or scavenging (SI-Fig. 5). However, statistical tests indicate that the mortality profile of Coc Muoi rhinocerotids, all taxa combined, is significantly different to the other profiles, *i.e.* Tam Hang, Duoi U'Oi, Sibrambang, Lida Ajer (73-63 ka, Westaway et al., 2017), and Punung (128-118 ka; Westaway et al., 2007) (Kolmogorov-Smirnov test, $p < 0.05$) (SI-Figs. 4–6).

In comparison with Coc Muoi, these sites include less adults and subadults and much more juveniles. These samples were somewhat biased by the action of scavengers and/or predators (Bacon et al., 2015), as shown for example in Fouvent-Saint-Andoche

(archetypical "hyena den"; Fourvel et al., 2014, 2015), in which the accumulation factor is primarily resulting from scavenging by hyenas. The rhinocerotid sample from Nam Lot (86% juveniles; 14% subadults) may be even more largely related to the action of the spotted hyena, whereas that of Sibrambang (58.6% juveniles; 9.3% subadults) may be related to the action of the tiger.

It is evident that at Coc Muoi the predator signature was different. The death pattern suggests that tigers (180–245 kg) might have selected individuals according to their chance encounter, and in the rich Coc Muoi ungulate community, tigers might have selected the largest ones (Schaller, 1967; Karanth and Sunquist, 1995; Biswas and Sankar, 2002; Bagchi et al., 2003; Andheria et al., 2007; Linki and Ridout, 2011; Hayward et al., 2012; Selvan et al., 2013; Lovari et al., 2015).

Fig. 12 demonstrates two separate clusters [Chitwan – Coc Muoi – Duoi U'Oi: *Rhinoceros*-dominated] and [Sibrambang – Lida Ajer – Punung; *Dicerorhinus*-dominated] (SI-Table 19). Fouvent-Saint-Andoche (with *Coelodonta antiquitatis*) may be connected to the latter cluster, as its similarity with Lida Ajer and Punung is not fully discarded (Khi-2; $0.001 < p < 0.05$). Tam Hang and Nam Lot are distinct from all other localities, with particularly no adult rhinoceros preserved (juveniles widely overrepresented) in the latter site.

Whether juvenile elephants were potential prey of tigers at Co Muoi remains an open question. However, one can note that, in comparison with the Duoi U'Oi population of elephants that of Coc Muoi includes very young juveniles (SI-Table 20).

Marks of enamel hypoplasia were common defects in mammals in the past, and they can be used as ecological indicators for a given period (Dobney and Ervynck, 2000; Niven et al., 2004; Skinner et al., 2016). With regard to the Indochinese region studied here, rates are to be compared between faunas referred to various climatic stages MIS6-5 (Coc Muoi: 148-117 ka), MIS5-4 (Tam Hang, Laos: 94-60 ka), MIS5 (Nam Lot, Laos: 86-72 ka), and MIS4 (Duoi U'Oi: 70-60 ka). Assessment of the health status of Coc Muoi rhinocerotids points to more stressful conditions than in any other Indochinese locality (SI-Table 21). Indeed, the rate of hypoplasia (26.8%) is higher than those calculated for the Tam Hang (0%), Duoi U'Oi (11.5%), and Nam Lot rhinocerotid samples (15.4%). The Coc Muoi individuals were exposed to physiological stress specific to age (weaning and abandonment of calf) combined with other environmental factors. The weaning age in rhinocerotids appears particularly critical as it shows the high rate of mortality in the concerned cohort [IV] (Fig. 11). In the woolly rhinocerotid sample from Fouvent-Saint-Andoche (Fourvel et al., 2015), the amount of EEH (~25%; pers. Obs. POA) is comparable to that of the rhinocerotid sample from Coc Muoi (26.8%). This French locality, located at mid-latitudes, experienced temperate-periglacial conditions during the Late Pleistocene. It is further referred to MIS3 (30–60 ka; Fourvel et al., 2014), a cold interval immediately preceding the last glacial maximum (26.5–19 ka; Clark et al., 2009). This period is characterized by harsh climatic conditions at mid- and high latitudes, which may easily explain the severe physiological stress observed in woolly rhinoceroses. Nevertheless, although these periglacial conditions have nothing in common with the local/regional environment as hypothesized for northern Vietnam by the time of deposition of the Coc Muoi assemblage, our data emphasize comparable levels of stress in rhinocerotid populations. Cheng et al. (2016) demonstrated that, in Asia, glacial terminations were followed by important variations of Asian monsoons. The age range of the Coc Muoi fauna, i.e. late Middle Pleistocene, was marked in south China by the strengthening of the East Asian summer monsoon ($\delta^{18}O$ data from Tantang cave; Li et al., 2017). Under its influence, the climate was particularly warm and humid with most likely a great variation in seasonal rainfalls (Ao et al., 2012). As such, rhinocerotids likely prove to be highly relevant as markers of locally instable/deteriorated environmental conditions, for a wide array of latitudes, climates, environments, and geological ages (see also Mead, 1999).

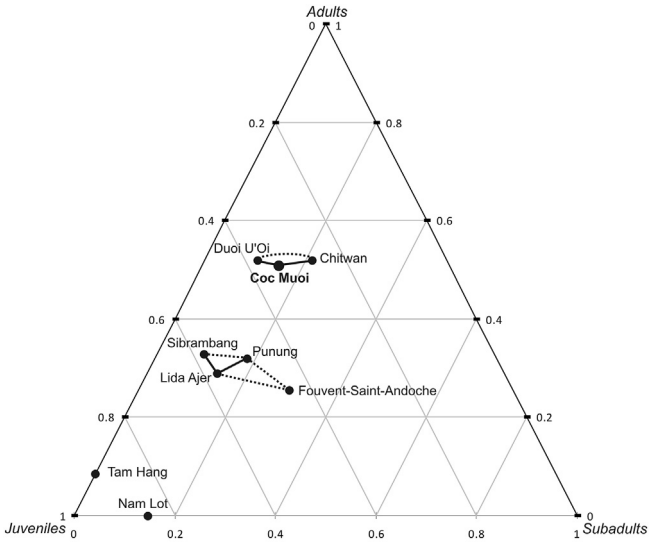

Fig. 12. Population structure comparison between selected Late Pleistocene rhinocerotid samples and a recent *Rhinoceros unicornis* natural population (Chitwan Park; Laurie et al., 1983). Fouvent-Saint-Andoche is a Late Pleistocene hyena den from France (30–60 kya; Fourvel et al., 2014). Solid lines: sample similarity not rejected ($p > 0.05$); dashed lines: sample similarity rejected ($0.001 < p < 0.05$); no line: sample similarity rejected ($p < 0.001$).

The percentage of Coc Muoi bovid teeth displaying enamel hypoplasia (15.9%) is higher than that calculated for Tam Hang (10.3%) and Nam Lot (0%), and demonstrates that this group was also exposed to a relatively higher degree of undernutrition and disease or other abiotic factors, during postnatal events (Niven et al., 2004) (SI-Table 22). Contrastingly, tapir teeth from Coc Muoi do not show any enamel defects coinciding with EEH.

6. Conclusions

The Coc Muoi data show that the ecosystem during MIS6-5 in northern Vietnam was shaped by diverse and abundant mega-herbivores, up to 5000 kg. At Coc Muoi specifically, tigers had access to a large population of rhinoceroses (*Rh. sondaicus*) in a forested vegetation with most likely more open areas and also canopied woodland. The health status of large-bodied herbivores (kouprey and rhinoceros) reveals the importance of stressors (biotic and abiotic) in a rainforest context, submitted most likely to important variations in the intensity of Asian monsoons. These Middle to Late Pleistocene ecosystems which occurred at these latitudes in Southeast Asia (23°-20°N) have no equivalent today with any ecosystems in Asia.

Acknowledgments

We thank all members of the Institute of Archaeology in Hanoi, and particularly Ass. Prof. Tong Trung Tin, Director of the Institute. We thank also all members of the Lang Son museum. The Institute of Archaeology (Nguyen Giang Hai, Nguyen Thi Mai Huong), the University of Macquarie (K. Westaway), the laboratory UPR2147 Dynamique de l'Evolution humaine (A.-M. Bacon), and the University of Strasbourg (Ph. Duringer, J.-L. Ponche), provided funding for the excavation and study of the Coc Muoi site. Kira Westaway's geochronological contribution is supported by a Discovery grant (DP1093049) from the Australian Research Council (ARC).

Appendix A. Supplementary data

Supplementary data related to this article can be found at https://doi.org/10.1016/j.quascirev.2018.02.017.

References

Andheria, A.P., Karanth, K.U., Kumar, N.S., 2007. Diet and prey profiles of three sympatric large carnivores in Bandipur Tiger reserve, India. J. Zool., Lond 273, 169–175.

Antoine, P.-O., 2012. Pleistocene and holocene rhinocerotids (mammalia, perissodactyla) from the Indochinese peninsula. C. R. Palevol 11, 159–168.

Ao, H., Dekkers, M.J., Xiao, G., Yang, X., Qin, L., Liu, X., Qiang, X., Chang, H., Zhao, H., 2012. Different orbital rythms in the Asian summer monsoon records from the North and South China during the Pleistocene. Global Planet. Change 80, 51–60.

Bacon, A.-M., Demeter, F., Schuster, M., Vu The, Long, Nguyen Kim, Thuy, Antoine, P.-O., Sen, S., Ha Huu, Nga, Nguyen Mai, Huong, 2004. The pleistocene Ma U'Oi cave, northern Vietnam: palaeontology, sedimentology, and palaeoenvironments. Geobios 37, 305–314.

Bacon, A.-M., Demeter, F., Duringer, P., Helm, C., Bano, M., Vu The, Long, Nguyen Kim, Thuy, Antoine, P.-O., Bui Thi, Mai, Nguyen Thi Mai, Huong, Dodo, Y., Chabaux, F., Rihs, S., 2008a. The Late Pleistocene Duoi U'Oi cave in northern Vietnam: palaeontology, sedimentology, taphonomy, palaeoenvironments. Quat. Sci. Rev. 27, 1627–1654.

Bacon, A.-M., Demeter, F., Tougard, C., de Vos, J., Sayavongkhamdy, T., Antoine, P.-O., Bouasisengpaseuth, B., Sichanthongtip, P., 2008b. Redécouverte d'une faune pléistocène dans les remplissages karstiques de Tam Hang au Laos : premiers résultats. C. R. Palevol 7, 277–288.

Bacon, A.-M., Duringer, P., Antoine, P.-O., Demeter, F., Shackelford, L., Sayavongkhamdy, T., Sichanthongtip, P., Khamdalavong, P., Nokhamaomphu, S., Sysuphanh, V., Patole-Edoumba, E., Chabaux, F., Pelt, E., 2011. The Middle Pleistocene mammalian fauna from Tam Hang karstic deposit, northern Laos: new data and evolutionary hypothesis. Quat. Int. 245, 315–332.

Bacon, A.-M., Demeter, F., Duringer, P., Patole-Edoumba, E., Sayavongkhamdy, T., Coupey, A.-S., Shackelford, L., Westaway, K., Ponche, J.-L., Antoine, P.-O., Sichanthongtip, P., 2012. Les sites de Tam Hang, Nam Lot et Tam Pà Ling au nord du Laos. Des Gisements à vertébrés aux origines des Hommes modernes, CNRS, Paris.

Bacon, A.-M., Westaway, K., Antoine, P.O., Duringer, P., Blin, A., Demeter, F., Ponche, J.-L., Zhao, J.-x., Barnes, L., Sayavongkhamdy, T., Nguyen Thi Kim, Thuy, Patole-Edoumba, E., Vu The, Long, Shackelford, L., 2015. Late Pleistocene mammalian assemblages of Southeast Asia: new dating, mortality profiles and evolution of the predator-prey relationships in an environmental context. Palaeogeogr. Palaeoclimatol. Palaeoecol. 422, 101–127.

Bae, J.C., Wang, W., Zhao, J., Huang, S., Tian, F., Shen, G., 2014. Modern human teeth from late Pleistocene Luna cave (Guangxi), China. Quat. Int. 354, 169–183.

Bagchi, S., Goyal, S.P., Sankar, K., 2003. Prey abundance and prey selection by tigers (*Panthera tigris*) in a semi-arid, dry forest in western India. J. Zool., Lond 260, 285–290.

Biswas, S., Sankar, K., 2002. Prey abundance and food habit of tigers (*Panthera tigris tigris*) in Pench National Park, Madhya Pradesh, India. J. Zool., Lond 256, 411–420.

Bocherens, H., Schrenk, F., Chaimanee, Y., Kullmer, O., Mörike, D., Pushkina, D., Jaeger, J.-J., 2017. Flexibility of diet and habitat in Pleistocene South Asian mammals: implications for the fate of the giant fossil ape *Gigantopithecus*. Quat. Int. 434, 148–155.

Brain, C.K., 1981. The Hunters and the Hunted? an Introduction to African Cave Taphonomy. The University of Chicago press, Chicago and London.

Bunn, H.T., Pickering, T.R., 2010. Methodological recommendations for ungulate mortality analyses in paleoanthropology. Quat. Res. 74, 388–394.

Buylaert, J.P., Murray, A.S., Thomsen, K.J., Jain, M., 2009. Testing the potential of an elevated temperature IRSL signal from K-feldspar. Radiat. Meas. 44, 560–565.

Cai, Y., Qiang, X., Wang, X., Jin, C., Wang, Y., Zhang, Y., Trinkaus, E., An, Z., 2017. The age of human remains and associated fauna from Zhiren Cave in Guangxi, southern China. Quat. Int. 434, 84–91.

Chen, G., Wang, W., Mo, J., Huang, Z., Tian, F., Huang, W., 2002. Pleistocene vertebrate fauna from Wuyun cave of Taindong county. Guangxi. Vertebrata PalAsiatica 40, 42–51.

Chen, S.K., Pang, L.B., He, C.D., Wei, G.B., Huang, W.B., Yue, Z.Y., Zhang, X.H., Zhang, H., Qin, L., 2013. New discoveries from the classic Quaternary mammalian fossil area of Yanjinggou, Chongqing, and their chronological explanations. Chin. Sci. Bull. 58, 3780–3787.

Cheng, H., Edwards, R.L., Sinha, A., Spötl, C., Yi, C., Chen, S., Kelly, M., Kathayat, G., Wang, X., Li, X., Kong, X., Wang, Y., Ning, Y., Zhang, H., 2016. The Asian Monsoon over the past 640,000 years and ice age terminations. Nature 534, 640–646.

Ciochon, R.L., 2009. The mystery ape of Pleistocene Asia. Nature 459, 910–911.

Ciochon, R.L., Olsen, J.W., 1986. Paleoanthropological and archaeological research in the socialist Republics of Vietnam. J. Hum. Evol. 15, 623–633.

Ciochon, R.L., Olsen, J.W., 1991. Paleoanthropological and archaeological discoveries from Lang Trang caves: a new middle Pleistocene hominid site from northern Viet-Nam. Indo-pacific prehistory assn. Bulletin 10, 59–73.

Ciochon, R.L., Long, V.T., Larick, R., Gonzalez, L., Grün, R., de Vos, J., Yonge, C., Taylor, L., Yoshida, H., Reagan, M., 1996. Dated co-occurrence of *Homo erectus* and *Gigantopithecus* from Tham Khuyen cave. Vietnam. Proc. Natl. Acad. Sci. USA 93, 3016–3020.

Clark, P.U., Dyke, A.S., Shakun, J.D., Carlson, A.E., Clark, J., Wohlfarth, B., Mitrovica, J.X., Hostetler, S.W., McCabe, A.M., 2009. The last glacial maximum. Science 325, 710–714.

Colbert, E.H., Hooijer, D.A., 1953. Pleistocene mammals from the limestone fissures of Szechwan, China. Bull. Amer. Mus. Nat. Hist 102, 1–134.

Corbet, G.B., Hill, J.E., 1992. The Mammals of the Indomalayan Region. Natural History Museum Publications. Oxford University Press.

Cuong, N.L., 1985. Fossile Menschenfunde aus Nordvietnam. In: Herrmann, J., Ullrich, H. (Eds.), Menschwerdung - Biotischer und gesellschaftlicher Entwicklungsprozess. Akademieverlag, Berlin, pp. 96–102.

Cuong, N.L., 1992. A reconsideration of the chronology of hominid fossils in Vietnam. In: Akazawa (Ed.), The evolution of dispersion of hominids in Asia 321–335.

Deprat, J., Giraud, J., Jacob, C., Mansuy, H., Bourret, R., Patte, E., Fromaget, J., 1963. Carte géologique au 1 : 500 000 de Cao Bang Est. Service géographique national du Viet Nam.

de Vos, J., Long, Vu The, 1993. Systematic Discussion of the Lang Trang Fauna (Unpublished report).

Dobney, K., Ervynck, A., 2000. Interpreting developmental stress in archaeological pigs: the chronology of linear enamel hypoplasia. J. Archaeol. Sci. 27, 597–607.

Duringer, P., Bacon, A.-M., Sayavongkhamdy, T., Nguyen Thi Kim, Thuy, 2012. Karst development, breccias history, and mammalian assemblages in Southeast Asia: a brief review. C. R. Palevol 11, 133–157.

Fourvel, J.-B., Fosse, P., Fernandez, P., Antoine, P.-O., 2014. La grotte de Fouvent, dit l'Abri Cuvier (Fouvent-le-Bas, Haute-Saône, France) : analyse taphonomique d'un repaire d'hyènes du Pléistocène supérieur (OIS 3). Paléo 25, 79–99.

Fourvel, J.-B., Fosse, P., Fernandez, P., Antoine, P.-O., 2015. Large mammals of fouvent (Haute-Saône, France): a glimpse into a late Pleistocene hyena den. Geodiversitas 37, 237–266.

Filoux, A., Wattanapituksakul, A., Lespes, C., Thongcharoenchaikit, 2015. A Pleistocene mammal assemblage containing *Ailuropoda* and *Pongo* from Tham Prakai Phet cave, Chaiyaphum province, Thailand. Geobios 48, 341–349.

Francis, C.M., 2008. A Field Guide to the Mammals of South-east Asia. New Holland Publishers, London.

Fromaget, J., 1931. L'Anthracolithique en Indochine après la régression moscovienne, ses transgressions et sa stratigraphie. Impr. d'Extrême-Orient.

Goodman, A.H., Rose, J.C., 1990. Assessment of systemic physiological perturbations from dental enamel hypoplasias and associated histological structures. Yearbk. Phys. Anthropol. 33, 59–110.

Grant, A., 1982. The use of tooth wear as a guide to the age of domestic ungulates. In: Wilson, B., Grigson, C., Payne, S. (Eds.), Ageing and Sexing Animal Bones from Archaeological Sites, BAR British Series 109, pp. 91–108.

Guérin, C., 1980. Les rhinocéros (Mammalia, Perissodactyla) du Miocène terminal au Pléistocène supérieur en Europe occidentale. Comparaison avec les espèces actuelles. Documents du laboratoire de géologie de Lyon. Sci. Terre 79 (3 fasc.), 1185.

Harrison, T., Jin, C., Zhang, Y., Wang, Y., Zhu, M., 2014. Fossil *Pongo* from the early Pleistocene *Gigantopithecus* fauna of Chongzuo, Guangxi, southern China. Quat. Int. 354, 59–67.

Hayward, M.W., Jedrzejewski, W., Jedrzewska, B., 2012. Prey preferences of the tiger *Panthera tigris*. J. Zool., Lond 286, 221–231.

Heintz, E. Les Cervidés villafranchiens de France et d'Espagne, Mémoires du Muséum, national d'Histoire naturelle, série C, Sciences de la Terre, XXII, vol. 1, 304 pages.

Hillman-Smith, A.K.K., Owen-Smith, N., Anderson, J.L., Hall-Martin, A.J., Selaladi, J.P., 1986. Age estimation of the White rhinoceros (*Ceratotherium simum*). J. Zool., Lond 210, 355–379.

Hillson, S., 2005. Teeth. In: Cambridge Manuals in Archaeology, second ed. Cambridge University Press. 373 pages.

Hooijer, D.A., 1946. Prehistoric and fossil rhinoceroses from the malay archipelago and India. Zool. Med. Leiden 26, 1–138.

Hooijer, D.A., 1948. Prehistoric Teeth of Man and the Orang-utan from Central Sumatra, with notes on the Fossil Orang-utan from Java and Southern China. Zool. Meded. Leiden 29, 175–301.

Jin, C., Wang, Y., Deng, C., Harrison, T., Qin, D., Pan, W., Zhang, Y., Zhu, M., Yan, Y., 2014. Chronological sequence of the early Pleistocene *Gigantopithecus* faunas from cave sites in the Chongzuo, Zuojiang river area, south China. Quat. Int. 354, 4–14.

Johnsingh, A.J.T., 1992. Prey selection in three large sympatric carnivores in Bandipur. Mammalia 56, 517–526.

Karanth, K.U., Sunquist, M.E., 1995. Prey selection by tiger, leopard and dhole in tropical forests. J. Anim. Ecol. 64, 439–450.

Kha, L.T., 1976. First remarks on the Quaternary fossil fauna of northern Vietnam. Vietnam. Stud. 46, 107–126.

Klein, R.G., 1978. Stone Age predation on large African bovids. J. Archaeol. Sci. 5, 195–217.

Laurie, W.A., Lang, E.M., Groves, C.P., 1983. Rhinoceros unicornis. Mamm. Species 211, 1–6.

Lekagul, B., McNeely, J.A., 1977. Mammals of Thailand. Association for the Conservation of the Wildlife, Bangkok.

Lenoble, A., Zeitoun, V., Laudet, F., Seveau, A., Doyasa, T., 2006. Natural processes involved in the formation of Pleistocene bone assemblages in continental South-East Asian caves: the case of the cave of the monk (Chiang Dao Wildlife

Sanctuary, Thailand). In: Pautreau, J.-P., Coupey, A.-S., Zeitoun, V., Rambault, E. (Eds.), 11th International Conference of the Eurasea, Septembre 2006. Siam Ratana Ltd, Chiang Mai, Bougon, France, pp. 41–50.
Leslie Jr., D.M., 2011. *Rusa unicolor* (artiodactyla: Cervidae). Mamm. Species 43, 1–30.
Li, B., Li, S.H., 2011. Luminescence dating of K-feldspar from sediments: a protocol without anomalous fading correction. Quat. Geochronol. 6, 468–479.
Li, B., Li, S.H., 2012. Luminescence dating of Chinese loess beyond 130 ka using the non-fading signal from K-feldspar. Quat. Geochronol. 10, 24–31.
Li, D., Hu, C., Wang, W., Chen, J., Tian, F., Huang, S., Bae, C.J., 2017. The stable isotope record in cervid tooth enamel from Tantang cave, Guangxi: implications for the Quaternary East Asian monsoon. Quat. Int. 434, 156–162.
Liu, W., Wu, X., Pei, S., Wu, X., Norton, C.J., 2010a. Huanglong cave: a late Pleistocene human fossil site in Hubei province, China. Quat. Int. 211, 29–41.
Liu, W., Jin, C.-Z., Zhang, Y.-Q., Cai, Y.-J., Xing, S., Wu, X-j., Cheng, H., Edwards, R.L., Pan, W.-S., Qin, D.-G., An, Z.-S., Trinkaus, E., Wu, X.-Z., 2010b. Human remains from Zhirendong, south China, and modern human emergence in East Asia. Proc. Natl. Acad. Sci. Unit. States Am. 107, 19201–19206.
Linkie, M., Ridout, M.S., 2011. Assessing tiger-prey interactions in Sumatran rainforests. J. Zool., Lond 284, 224–229.
Liu, W., Martinon-Torres, M., Cai, Y.-j., Xing, S., Tong, H.-w., Pei, S.-w., Sier, M.J., Wu, X.-h., Edwards, R.L., Cheng, H., Li, Y.-y., Yang, X.-x., Bermudez de Castro, J.M., Wu, X.-j., 2015. The earliest unequivocally modern humans in southern China. Nature 526, 696–699.
Long, V.T., Du, H.V., 1981. Zoological species belonging to the Pleistocene and the geochronology of sediments containing them in caves and grottos in Northern Viet Nam. Khao Co Hoc 1, 16–19 (in Vietnamese).
Long, V.T., de Vos, J., Ciochon, R.S., 1996. The fossil mammal fauna of the Lang Trang caves, Vietnam, compared with Southeast Asian fossil and recent mammal faunas: the geographical implications. Bulletin of the Indo-Pacific Prehistory Association 14, 101–109.
Lovari, S., Pokheral, C.P., Jnawali, S.R., Fusani, L., Ferretti, F., 2015. Coexistence of the tiger and the common leopard in a prey-rich area: the role of key partitioning. J. Zool., Lond 295, 122–131.
Louys, J., Meijaard, E., 2010. Palaeoecology of Southeast Asian megafauna-bearing sites from the Pleistocene and a review of environmental changes in the region. J. Biogeogr. 37, 1432–1449.
Lyman, R.L., 1994. Vertebrate Taphonomy. Cambridge University Press, 524p.
Lyman, R.L., 2008. Quantitative Paleozoology. Cambridge University Press, 348p.
Ma, J., Wang, Y., Jin, C., Yan, Y., Qu, Y., Hu, Y., 2017. Isotopic evidence of foraging ecology of Asian elephant (*Elephas maximus*) in South China during the Late Pleistocene. Quat. Int. 443, 160–167.
Mead, A.J., 1999. Enamel hypoplasia in Miocene rhinoceroses (*Teleoceras*) from Nebraska: evidence of severe physiological stress. J. Vertebr. Paleontol. 19, 391–397.
Maglio, V.J., 1973. Origin and evolution of the elephantidae. Trans. Am. Phil. Soc. 63 (part 3), 149p.
Niven, L.B., Egeland, C.P., Todd, L.C., 2004. An inter-site comparison of enamel hypoplasia in bison: implications for paleoecology and modeling Late Plains Archaic subsistence. J. Archaeol. Sci. 31, 1783–1784.
Norton, C.J., Jin, C., Wang, Y., Zhang, Y., 2010. Rethinking the Paleartic-Oriental biogeographic boundary in quaternary China. In: Norton, C.J., Braun, D.R. (Eds.), Asian Paleoanthropology: from Africa to China and beyond. Vertebrate Paleobiology and Paleoanthropology, pp. 81–100.
Nowak, R.M., 1999. Walker's Mammals of the World, sixth ed., vol. I. The Johns Hopkins University Press, Baltimore and London.
Olsen, J.W., Ciochon, R.L., 1990. A review of evidence for postulated Middle Pleistocene occupations in Viet Nam. J. Hum. Evol. 19, 761–788.
Pei, W.C., 1935. Fossil mammals from the Kwangsi caves. Bull. Geol. Surv. Can. 14, 413–425.
Ramesh, T., Sankar, K., Qureshi, Q., Kalle, R., 2012. Group size, sex and age composition of chital (*Axis axis*) and sambar (*Rusa unicolor*) in a deciduous habitat of Western Ghats. Mamm. Biol. 77, 53–59.
R Core Team, 2017. R: a Language and Environment for Statistical Computing. R Foundation for Statistical Computing, Vienna, Austria. http://www.R-project.org/.
Rink, W.J., Wang, W., Bekken, D., Jones, H.L., 2008. Geochronology of *Ailuropoda-Stegodon* fauna and *Gigantopithecus* in Guangxi province. Quat. Res. 69, 377–387.
Roth, V.L., Shoshani, J., 1988. Dental identification and age determination in *Elephas maximus*. J. Zool., Lond 214, 567–588.
Rolett, B.V., Chiu, M., 1994. Age estimation of prehistoric pigs (*Sus scrofa*) by molar eruption and attrition. J. Archaeol. Sci. 21, 377–386.
Schaller, G.B., 1967. The Deer and the Tiger. A Study of Wildlife in India. The University of Chicago Press, 370 p.
Schwartz, J.H., Long, V.T., Cuong, N.L., Kha, L.T., Tattersall, I., 1994. A diverse hominoid fauna from the late middle Pleistocene breccia cave of Tham Kuyen, Socialist Republic of Vietnam. Anthropol. Pap. Am. Mus. Nat. Hist. 74, 1–11.
Schwartz, J.H., Long, V.T., Cuong, N.L., Kha, L.T., Tattersall, I., 1995. A review of the Pleistocene hominoid fauna of the Socialist Republic of Vietnam. Anthropol. Pap. Am. Mus. Nat. Hist. 76, 1–24.
Selvan, K.M., Veeraswami, G.G., Lyndoh, S., Habib, B., Hussain, S.A., 2013. Prey selection and food habits of three sympatric large carnivores in a tropical lowland forest of the Eastern Himalayan biodiversity hotspot. Mamm. Biol. 78, 296–303.
Shen, G., Wang, W., Wang, Q., Zhao, J., Collerson, K., Zhou, C., Tobias, P.V., 2002. U-series dating of Liujiang hominid site in Guangxi, Southern China. J. Hum. Evol. 43, 817–829.
Skinner, M.F., Skinner, M.M., Pilbrow, V.C., Hannibal, D.L., 2016. An enigmatic hypoplastic defect of the maxillary lateral incisor in recent and fossil orangutans from Sumatra (*Pongo abelii*) and Borneo (*Pongo pygmaeus*). Int. J. Primatol. 37, 548–567.
Steele, T.E., 2004. Variation in mortality profiles of red deer (*Cervus elaphus*) in Middle Paleolithic assemblages from Western Europe. Int. J. Osteoarchaeol. 14, 304–320.
Stiner, M.C., 1990. The use of mortality patterns in archaeological studies of hominid predatory adaptations. J. Anthropol. Archaeol. 9, 305–351.
Stiner, M.C., 1998. Mortality analysis of Pleistocene bears and its paleoanthropological relevance. J. Hum. Evol. 34, 303–326.
Storm, P., de Vos, J., 2006. Rediscovery of the late Pleistocene Punung hominin sites and the discovery of a new site Gunung Dawung in east Java. Senckenberg. Lethaea 86 (2), 121–131.
Suckling, G., 1989. Developmental defects of enamel - historical and present-day perspectives of dental enamel. Adv. Dent. Res. 3, 87–94.
Suraprasit, K., Jaeger, J.-J., Chaimanee, Y., Chavasseau, O., Yamee, C., Tian, P., Panha, S., 2016. The middle Pleistocene fauna from Khok Sung (Nakhon Ratchasima, Thailand): biochronological and paleobiogeographical implications. ZooKeys 613, 1–157.
Takai, M., Zhang, Y., Kono, R.T., Jin, C., 2014. Changes in the composition of the Pleistocene primate fauna in southern China. Quat. Int. 354, 75–85.
Thiel, C., Buylaert, J.-P., Murray, A., Terhorst, B., Hofer, I., Tsukamoto, S., Frechen, M., 2011. Luminescence dating of the Stratzing loess profile (Austria) – testing the potential of an elevated temperature post-IR IRSL protocol. Quat. Int. 234, 23–31.
Thompsen, K.J., Murray, A.S., Jain, M., Botter-Jensen, L., 2008. Laboratory fading rates of various luminescence signals from feldspar-rich sediment extracts. Radiat. Meas. 43, 1474–1486.
Thein, Tin, 1974. La faune néolithique du Phnom Loang (Cambodge) (Ruminants). Doctorat de 3ème cycle de l'Université Paris VI.
Tong, H.W., 2005. Dental characters of the Quaternary tapirs in China, their significance in classification and phylogenetic assessment. Geobios 38, 139–150.
Tong, H.W., Zhang, S., Chen, F., Li, Q., 2008. Rongements sélectifs des os par les porcs-épics et autres rongeurs : cas de la grotte de Tianyuan, un site avec des restes humains fossiles récemment découverts près de Zhoukoudian (Choukoutien). L'Anthropologie 112, 353–369.
Tong, H.W., Guérin, C., 2009. Early Pleistocene *Dicerorhinus sumatrensis* remains from the Liucheng *Gigantopithecus* cave, Guangxi, China. Geobios 42, 525–539.
Tougard, C., 1998. Les faunes de grands mammifères du Pléistocène moyen terminal de Thaïlande dans leur cadre phylogénétique, paléoécologique et biochronologique. Thèse de Doctorat. Université de Montpellier II.
Tougard, C., 2001. Biogeography and migration routes of large mammal faunas in South-East Asia during the Late Middle Pleistocene: focus on the fossil and extant faunas from Thailand. Palaeogeogr. Palaeoclimatol. Palaeoecol. 168, 337–358.
Tougard, C., Montuire, S., 2006. Pleistocene paleoenvironmental reconstructions and mammalian evolution in South-East Asia: focus on fossil faunas from Thailand. Quat. Sci. Rev. 25, 126–141.
Turvey, S.T., Tong, H., Stuart, A.J., Lister, A.M., 2013. Holocene survival of Late Pleistocene megafauna in China: a critical review of the evidence. Quat. Sci. Rev. 76, 156–166.
van Valkenburgh, B., 1988. Trophic diversity in past and present guilds of large predatory mammals. Paleobiology 14, 155–173.
van Valkenburgh, B., Hertel, F., 1993. Tough times at La Brea: tooth breakage in large carnivores of the Late Pleistocene. Science 261, 456–459.
van Valkenburgh, B., Hayward, M.W., Ripple, W.J., Meloro, C., Roth, V.L., 2016. The impact of large terrestrial carnivores on Pleistocene ecosystems. Proc. Natl. Acad. Sci. U.S.A. 113, 862–867 .
Van den Bergh, G.D., 1999. The Late Neogene elephantoid-bearing faunas of Indonesia and their palaeozoogeographic implications. A study of the terrestrial faunal succession of Sulawesi, Flores and Java, including evidence for early hominid dispersal east of Wallace's Line. Scripta Geol. 117, 1–419.
Wang, W., Potts, R., Baoyin, Y., Huang, W., Cheng, H., Edwards, R.L., Ditchfield, P., 2007. Sequence of mammalian fossils, including hominoid teeth, from the Bubing Basin caves, South China. J. Hum. Evol. 52, 370–379.
Wang, W., Liao, W., Li, D., Tian, F., 2014. Early Pleistocene large-mammal fauna associated with *Gigantopithecus* at Mohui cave, Bubing basin, south China. Quat. Int. 354, 122–130.
Westaway, K.E., Morwood, M.J., Roberts, R.G., Rokus, A.D., Zhao, J.X., Storm, P., Aziz, F., van den Bergh, G., Hadi, P., Jatmiko, de Vos, J., 2007. Age and biostratigraphic significance of the Punung rainforest fauna East Java, Indonesia, and implications for *Pongo* and *Homo*. J. Hum. Evol. 53, 709–717.
Westaway, K.E., Louys, J., Due Awe, D., Morwood, M.J., Price, G.J., Zhao, J-x., Aubert, M., Joannes-Boyau, R., Smith, T.M., Skinner, M.M., Compton, T., Bailey, R.M., van den Bergh, G.D., de Vos, J., Pike, A.W.G., Stringer, C., Saptomo, E.W., Rizal, Y., Zaim, J., Santoso, W.D., Trihascaryo, A., Kinsley, L., Sulisttyanto, B., 2017. An early modern human presence in Sumatra 73,000–63,000 years ago. Nature 548, 322–325.
Wilson, D.E., Reeder, D.M., 2005. Mammal Species of the World, a Taxonomic and Geographic Reference, third ed. The Johns Hopkins University press, Baltimore.
Yan, Y., Wang, Y., Jin, C., Mead, J.I., 2014. New remains of *rhinoceros* (Rhinocerotidae, perissodactyla, mammalia) associated with *Gigantopithecus blacki* from the

early Pleistocene Yanliang cave, Fusui, south China. Quat. Int. 354, 110–124.
Zhang, Y., Jin, C., Cai, Y., Kono, R., Wang, W., Wang, Y., Zhu, M., Yan, Y., 2014. New 400-320 ka *Gigantopithecus blacki* remains from Hejiang cave, Chongzuo city, Guangxi, south China. Quat. Int. 354, 35–45.
Zeitoun, V., Seveau, A., Forestier, H., Thomas, H., Lenoble, A., Laudet, F., Antoine, P.O., Debruyne, R., Ginsburg, L., Mein, P., Winayalai, C., Chumdee, N., Doyasa, T., Kijngam, A., Nakbunlung, S., 2005. Découverte d'un assemblage faunique à *Stegodon-Ailuropoda* dans une grotte du nord de la Thaïlande (Ban fa Suai, Chiang Dao). C. R. Palevol 4, 255–264.
Zheng, Z., Lei, Z.-Q., 1999. A 400,000 years record of vegetational and climatic changes from a volcanic basin, Leizhou Peninsula, southern China. Palaeogeogr. Palaeoclimatol. Palaeoecol. 145, 339–362.